Description of the Iodine Model AIM-3 in COCOSYS

Vorhaben RS 1159

Weiterentwicklung der Rechenprogramme COCOSYS und ASTEC

Technischer Bericht

GRS - A - 3508

Gesellschaft für Anlagen-
und Reaktorsicherheit
(GRS) mbH

**Technischer Bericht/
Technical Report**

Reaktorsicherheitsforschung-
Vorhabens Nr.:/
Reactor Safety Research-Project No.:
RS 1159

Vorhabenstitel / Project Title:
Weiterentwicklung der
Rechenprogramme
COCOSYS und ASTEC

Further development of the
simulation codes COCOSYS
and ASTEC

Berichtstitel:
Description of the Iodine Model AIM-3 in COCOSYS

Autor / Authors:
G. Weber
F. Funke *
*AREVA NP, Erlangen

Berichtszeitraum / Publication Date:
November 2009

Anmerkung:

Das diesem Bericht zugrunde liegende F&E-Vorhaben wurde im Auftrag des Bundesministeriums für Wirtschaft und Technologie (BMWi) unter dem Kennzeichen RS 1159 durchgeführt.

GRS - A - 3508

Abstract

AIM (**A**dvanced **I**odine **M**odel) is the iodine module in the **Co**ntainment **Co**de **Sys**tem COCOSYS. It simulates the iodine behaviour in a LWR containment during a severe accident. AIM calculates a total of 70 chemical reactions and physical processes for 26 iodine species and 8 non-iodine species in each compartment as well as the iodine transport between compartments by gas and water flows. The thermal hydraulic conditions are provided by the thermal hydraulic module and the aerosol behaviour of the particulate iodine species is treated by the aerosol module.

In this report all essential chemical iodine reactions in the liquid and gaseous phases and all physical processes (mass transfer, etc.) modelled in version **AIM-3** as well as the interfaces to other COCOSYS modules are described. The complete set of reaction rate constants and activation energies is given and the AIM input parameters are described.

Kurzfassung

AIM (**A**dvanced **I**odine **M**odule) ist der Iod-Modul im **Co**ntainment **Co**de **Sys**tem COCOSYS. Er simuliert das Iodverhalten in einem LWR-Containment während eines schweren Reaktorunfalls. AIM berechnet insgesamt 70 chemische Reaktionen und physikalische Prozesse für 26 Iodspezies und 8 weitere Spezies in jeder Rechenzone sowie den Iodtransport mit den Gas- und Wasserströmen zwischen den Räumen. Die thermohydraulischen Randbedingungen werden vom Thermohydraulikmodul zur Verfügung gestellt und das Aerosolverhalten der partikelförmigen Iodspezies wird im Aerosolmodul berechnet.

In diesem Bericht sind alle in **AIM-3** modellierten chemischen Iodreaktionen in der Gas- und Wasserphase, die erfassten physikalischen Prozesse (Massentransfer, etc.) sowie die Schnittstellen zu anderen COCOSYS-Modulen beschrieben. Auch ist der komplette Satz der Reaktionskonstanten und Aktivierungsenergien wiedergegeben und die AIM Eingabegrößen sind beschrieben.

Contents

List of Tables

List of Figures

1 Introduction 1

2 Iodine species and their physical behaviour 3

2.1 Overview of species 3

2.2 Physical behaviour 7

3 Iodine reaction processes 10

3.1 Rate constants and temperature dependence 10

3.2 Water phase reactions 11

3.2.1 Inorganic iodine hydrolysis reactions 11

3.2.2 Inorganic iodine radiolysis reactions 14

3.2.3 Silver / iodine reactions 16

3.2.4 Organic iodine reactions in the homogeneous phase 20

3.2.5 Iodine reactions with immersed painted surfaces 22

3.2.6 Iodine reaction with immersed steel surface 28

3.2.7 Iodine reactions with immersed, bare concrete surfaces 28

3.3 Gas phase reactions 29

3.3.1 Iodine / ozone reaction 29

3.3.2 Organic iodide destruction in the gas phase 32

3.3.3 Iodine reactions with painted surfaces exposed to the gas phase 33

3.3.4 Iodine reactions with steel surfaces exposed to the gas phase 39

3.3.5 Iodine reactions with bare concrete surfaces exposed to the gas phase .. 44

3.4 Interfacial mass transfer and aerosol processes 45

3.4.1 Mass transfer between gas and water phases at non-boiling conditions .. 45

3.4.2 Mass transfer between gas and water phases at boiling conditions 48

3.4.3 Iodine aerosol deposition and resuspension 49

4 Summary of iodine reaction data 53

5 Coupling within COCOSYS 60
5.1 Separate iodine nodalisation 60
5.2 Interactions with thermal hydraulics 62
5.2.1 Atmospheric iodine transport 62
5.2.2 Dry and wet conditions 63
5.2.3 Iodine wash-down 64
5.2.4 Removal by spray 65
5.3 Iodine aerosol behaviour 66
5.3.1 Well-mixed aerosol approach 68
5.3.2 Aerosol calculation in detail 69
5.3.3 Resuspension 70

6 Validation 73

7 Description of input parameters 75

8 Literature 81

9 Distribution List 89

List of Tables

Table 2-1: Iodine species in AIM-3 3

Table 3-1: Conditions covered by various CH_3I release tests..... 38

Table 4-1: Chemical and physical rate constants in the iodine model AIM-3 55

Table 5-1: Rules for a separate iodine nodalisation 61

Table 5-2: Model options for iodine aerosol treatment 66

Table 6-1: AIM validation matrix 73

Table 7-1: Input parameter description..... 75

List of Figures

Figure 3-1: Modelling of wet I_2 deposition on paint..... 35

Figure 5-1: Example for a separate iodine nodalisation (PHEBUS-FP containment)... 61

1 Introduction

In COCOSYS V2.4 the iodine behaviour is calculated by the semi-mechanistic iodine model AIM-3 (**A**dvanced **I**odine **M**odel, **3**rd version). AIM has been designed to simulate the iodine transport and behaviour in multi-compartment containment geometries. It is based on IMPAIR-3 /GÜN 92/. Numerous developments resulted in AIM-F2, the precursor version of AIM-3 /KLE 00/. Recent improvements stemming mainly from THAI iodine tests /FUN 04, WEB 05/ and also from other international projects are included in the present version AIM-3.

AIM calculates 52 chemical reactions and 18 physical processes in each compartment. A compartment may consist of a gas phase and a water phase (sump) or a gas phase only. The iodine transport between the compartments by gas and water flows is provided by the thermal hydraulic part of COCOSYS and the aerosol behaviour of the particulate iodine species is treated by the aerosol part. The impact of engineered systems (filter, spray, etc.) on the iodine behaviour is modelled.

With AIM it is possible to use a separate nodalisation which has less computational zones than the global (thermal hydraulic) nodalisation. In some iodine cases a reduced spatial resolution is appropriate, e.g. in the gas space above a large sump. Additionally computing time can be saved.

The main improvements of AIM-3 compared to previous versions concern:

- I_2 interaction with paint and steel based upon THAI data
- Release of organic iodide from paint in the gas and water phases
- I_2/ozone interaction and the aerosol behaviour of the particulate IO_3^- species
- Mass transfer of volatile species for boiling conditions

In this report all chemical reactions and physical processes modelled in AIM-3, the coupling of this iodine model to other modules in COCOSYS, and the AIM input parameters are described. Additionally the complete set of reaction rate constants and activation energies is given.

This model description include contributions provided by AREVA NP comprising information on numerous sub-models developed in various projects (e.g. BMBF project “Flüchtiges Iod” /FUN 99/, PARIS project /LAN 05/) and later incorporated into AIM. These contributions have not been subject of the BMWi project RS 1159. In particular, experimental studies, model restrictions, validation work and recommendations for application were provided. These important and extensive informations were checked by GRS and included in the AIM-3 description.

2 Iodine species and their physical behaviour

2.1 Overview of species

Twenty-six iodine species and eight non-iodine species are treated (Table 2-1). The iodine species comprise eight iodine compounds (I_2, I^-, IO_3^-, CH_3I, AgI, HOI; I_{FeI2} and I_{chs}). The species are associated with the following hosts:

- water phase (sump)
- immersed surfaces (paint, steel, concrete)
- gas phase
- surfaces exposed to the gas phase (paint, steel, concrete)
- aerosols (dry particles, droplets)

Ten iodine species are defined in the water phase and on the immersed surfaces and sixteen are defined in the gas phase and on the surfaces exposed to the gas phase. Additionally eight non-iodine species [Ag(w), AgO_X(w), CH_3(w), Boron(w), CH_3(g), O_3(g), Ag-aerosol(g), and Ag-aerosol-depos(g)] are balanced for the use in particular iodine reactions. Elements present in a large quantity, like O_2 or Fe, are not balanced. Boron is balanced in AIM but not used in the iodine model.

Table 2-1: Iodine species in AIM-3

Chemical name and state of species	Concentration variable in code, (output variable)	Dimension	Index of rate variable ZDOT[1]	Modelled molar mass (g/mol)
Gas phase				
I_2 (g) Gaseous molecular iodine	I2G (I2)	mol/l	1	258
I^- (g) CsI aerosols	IMINUSG (I-)	mol/l	2	129

[1] E.g. ZDOT(1) = d I2G /dt in mol/(l·s)

Chemical name and state of species	Concentration variable in code, (output variable)	Dimension	Index of rate variable ZDOT[1]	Modelled molar mass (g/mol)
IO_3^- (g) Iodate aerosol; representative for iodine oxides	IO3MING (IO3-)	mol/l	3	129
CH_3I (g) Organic iodides	CH3IG (RI)	mol/l	4	129
I_2 (dep,p,g) Physisorbed I_2 on paint	DEPGP (I2_PAINT)	mol/m²	5	258
AgI (g) Silver iodide aerosols	AGIG (AGI)	mol/l	6	129
I_2 (dep,s,g) Physisorbed I_2 on steel	DEPGS (I2_STEEL)	mol/m²	7	258
I_2 (dep,c,g) I_2 deposits on concrete	DEPGC (I2_CONCR)	mol/m²	8	258
I^- (droplets) Wet aerosol	IMINUSTR (I-_DROPS)	mol/l	9	129
IO_3^- (droplets) Wet aerosol	IO3TR (IO3-_DROPS)	mol/l	10	129
HOI (droplets) Hypoiodous acid; wet aerosol	HOITR (HOI)	mol/l	11	129
CH_3 (g) Organic residues	CH3G (R)	mol/l	12	CH_3: 15
O_3 (g) Ozone (radiolysis product)	O3G (O3)	mol/l	13	O_3: 48
Ag-aerosol (g)	AG_G (AG)	mol/l	14	Ag: 107.87
I_{FeI2} (dep,s,g) Representative for iodides chemisorbed on steel	DEPG_FEI2 (FEI2)	mol/m²	15	258
I_{chs} (dep,p,g) Chemisorbed on paint	DEPG_ICHS (ICHS_PAINT)	mol/m²	16	129
CsI aerosol deposits	CSI_AEDEP (CSI_AEDEP)	mol/m²	17	129

Chemical name and state of species	Concentration variable in code, (output variable)	Dimension	Index of rate variable ZDOT[1]	Modelled molar mass (g/mol)
IO_3^- aerosol deposits	IO3-_AEDEP (IO3-_AEDEP)	mol/m²	18	129
AgI aerosol deposits	AGI_AEDEP (AGI_AEDEP)	mol/m²	19	129
Ag-aerosol-depos (g)	AG_AEDEP (AG_AEDEP)	mol/m²	20	Ag: 107.87
Water phase				
I_2 (w) Dissolved molecular iodine	I2 (I2)	mol/l	MGZ+1 [2]	258
I^- (w) Dissolved iodide	IMINUS (I-)	mol/l	MGZ+2	129
IO_3^- (w) Dissolved iodate	IO3MIN (IO3-)	mol/l	MGZ+3	129
AgI (w) Suspended silver iodide particles	AGI (AGI)	mol/l	MGZ+4	129
CH_3I (w) Dissolved organic iodides	CH3I (RI)	mol/l	MGZ+5	129
Ag (w) Suspended silver particles	AG (AG)	mol/l	MGZ+6	Ag: 107.87
CH_3 (w) Dissolved organic residues	CH3 (R)	mol/l	MGZ+7	CH_3: 15
HOI (w) Dissolved hypoiodous acid	HOI (HOI)	mol/l	MGZ+8	129
I_2 (dep,p,w) Physisorbed I_2 on immersed paint	DEPWP (I2_PAINT)	mol/m²	MGZ+9	258
I_{chs} (dep,p,w) Chemisorbed I^- on immersed paint	DEPW_ICHS (ICHS_PAINT)	mol/m²	MGZ+10	129

[2] MGZ = number of gas phase species

Chemical name and state of species	Concentration variable in code, (output variable)	Dimension	Index of rate variable ZDOT[1]	Modelled molar mass (g/mol)
I_2 (dep,c,w) I_2 deposits on immersed concrete	DEPWC (I2_CONCR)	mol/m²	MGZ+11	258
I^- (dep,p,w) Physisorbed I^- on immersed paint	DEPWI (I-_PAINT)	mol/m²	MGZ+12	129
AgO_x (w) Silver oxide layer on suspended silver particles	AGOX (AGOX)	mol/l	MGZ+13	Ag: 107.87
Boron (w)	BORON (BORON)	mol/l	MGZ+14	B: 10.81

Organic iodides

In AIM the whole spectrum of volatile organic iodides is modelled by use of the collective term "CH_3I", in the gaseous and the water phases, respectively. This means, CH_3I in AIM stands not only for methyl iodide, but includes other highly volatile, generally lower weight organic iodides. Therefore the use of CH_3I means a certain averaging of different chemical and physico-chemical behaviour of the organic iodides combined. This procedure is in accordance to the underlying experimental database where frequently only the sum of all organic iodides, but no speciation was measured. In AIM CH_3I is equivalent to RI, the internationally commonly used term for organic iodides.

Attempts were made in the past, e.g. in IMPAIR /GÜN 92/, to further subdivide the organic iodides into two groups, the so-called lower-weight organic iodides ("CH3I") and higher-weight organic iodides ("HMWI"). However, the grouping into these two classes of volatility was somewhat arbitrary for the large range of organic iodides whose volatilities and chemical behaviour are changing continuously. It is difficult to derive mean chemical and physico-chemical process parameters for such classes from the experimental database. Therefore, the concept of only one class of volatile organic iodides has been introduced in AIM-3, and this class is denominated "CH_3I".

Dimensions

In AIM, concentrations in the homogeneous gas and water phases are defined in **mol/l**, surface deposits in **mol/m^2**. The output additionally indicates results in **grams**. Non-iodine elements are **not** considered in the iodine species mass, see Tab. 2-1, but for the aerosol behaviour (settling, etc.) of particulate iodine species the mass of non-iodine elements is regarded.

Surface and volumes are to be used in **m^2** and **m^3**, respectively. This requires "dimension factors" in reaction rates for volumetric concentrations in mol/l.

The time basis for reaction rates is **seconds**. The dose rates are to be used in **kGy/h**. The activation energies are given in **J/mol**.

Atomic weights

The average atomic weight of all fission product iodine isotopes is set to 129 g/mol, the respective molecular weight of elemental iodine (I_2) is 258 g/mol. Table 2-1 also provides molecular weights of other elements relevant for iodine modelling.

2.2 Physical behaviour

The physical behaviour of the iodine species, like their deposition behaviour, differs considerably within the containment under severe accident conditions. The main properties are summarized here.

In the gas phase

- **Elemental iodine (I_2)** is a reactive and water-soluble gas which deposits on and resuspends from surfaces. It is transferred, in both directions, between gas and water phases striving for concentration equilibrium. It is subject to many chemical reactions in both phases. An important sink for I_2 in a containment are the painted surfaces.
- **Cesium iodide (CsI(g))** and **iodate (IO_3^-(g))** as suspended in the gas phase are soluble iodine aerosols. They settle on floors and walls by deposition processes. Iodate aerosol is formed from I_2 by a gas-to-particle conversion.

- **Organic iodides (collective term: CH_3I)** are less reactive, volatile iodine species and contribute significantly to the iodine inventory in the gas phase. No deposition onto surfaces is modelled. As with I_2, CH_3I is transferred, in both directions, between gas and water phases.

In the water phase

- **I^-(w), HOI(w), IO_3^-(w)** are soluble iodine species in the water
- **AgI** is poorly soluble in water and thus represents an important iodine sink in PWRs using control rods made of SIC (= silver, indium, and cadmium), as the silver particles in the containment sump can react efficiently with iodine.
- **I_2(w) and CH_3I(w)** can dissolve to certain concentrations only (Henry's law). They are dissolved or gas out until an equilibrium with the gas phase concentration is reached.

Physico-chemical behaviour on surfaces

- **Painted surfaces** are an important sink for volatile I_2, because of an efficient and strong binding of deposited iodine by chemisorption. In AIM-3 the following iodine species on painted surfaces in the gas phase are distinguished:
  - physisorbed I_2 (DEPGP): I_2 weakly bound to the paint, can be resuspended or washed-down with wall condensation
  - chemisorbed iodine (DEPG_ICHS): iodine strongly bound to the paint, can be resuspended as organic iodide only or washed down as iodide
  - Iodine aerosol deposits (CsI_AEDEP, IO3-_AEDEP, AGI_AEDEP): do not take part in iodine chemistry processes on the surface, but in the sump if washed down
  - Aqueous iodine is deposited onto immersed painted surfaces and it can chemically react with the paint to non-soluble iodine
- **Steel surfaces** are also a sink for volatile iodine, but less efficient effects than painted surfaces. For iodine tests carried out in stainless steel vessels like THAI or PHEBUS-FP the surface reactions are of special interest. In a reactor containment the importance of the steel reaction is much less due to the small bare steel area. An exception can be the use of RMI (reflecting metal

insulation). The following iodine species on steel surfaces in the gas phase are distinguished in AIM-3:

- physisorbed I_2 (DEPGS): I_2 weakly bound to the steel surface, can be resuspended or washed-down by wall condensate
- chemisorbed iodine (DEPG_FEI2): iodine strongly bound to the steel surface, can be washed down as iodide
- Iodine aerosol deposits (CsI_AEDEP, IO3-_AEDEP, etc.): do not take part in iodine chemistry processes on the surface, but in the sump if washed down.

No iodine loading on immersed steel surfaces (DEPWS) is modelled due to the immediate dissolution of the iodine/steel reaction products.

3 Iodine reaction processes

In this chapter the modelling of chemical reactions and physical processes for iodine in AIM-3 are described. AIM-3 is the successor of AIM-F2 and AIM-F1, with the latter being described in the COCOSYS User Manual /KLE 00/. AIM-3 is substantially revised based upon results from recent THAI projects and from the outcomes of international projects such as ISP 41 /BAL 04/.

3.1 Rate constants and temperature dependence

AIM calculates the concentrations of the considered species resulting from a large number of coupled processes as function of time. Usual concepts of chemical reaction kinetics are applied. E. g., in a chemical equation of the general form

$$A + B \underset{k(2)}{\overset{k(1)}{\rightleftarrows}} C + D,$$

k(1) is the constant for the forward reaction and k(2) for the reverse reaction. The net reaction rate for species C is then for instance in a simple case:

$$\frac{d[C]}{dt} = k(1)\,[A]\,[B] - k(2)\,[C]\,[D] + S$$

[A] to [D] are the concentrations of the species. S is a source for species C, e.g. from injection.

A kinetic equation is formulated in AIM for each species defined in Table 2-1, except for boron. The resulting set of coupled, non-linear, ordinary differential equations is solved for each iodine zone. The iodine transport between the zones is treated quasi-stationary, i.e. the iodine mass flow is constant during a time step.

The reaction constants BAS_i are the kinetic constants at a temperature of 25 ^{0}C. The **Arrhenius equation** is mostly applied to calculate the rate constants at elevated temperatures.

$$k_i = BAS_i \cdot \exp\left[\ EAKT_i \left(\frac{T - 298.15}{T \cdot R \cdot 298.15} \right) \ \right]$$

$k_i = BAS_i$ at T = 25 °C

k_i	rate constant, different dimensions
T	temperature [K]
R	gas constant, = 8.3144 J/(mol·K)
$EAKT_i$	activation energy, J/mol

If the activation energy is set to zero in the input file, the reaction is generally regarded to be temperature independent. However, there are exceptions in some models where the activation energy is calculated within the model and any input activation energy value is ignored, e.g. for the kinetic constant k(12) of the reverse hydrolysis step 1.

For the deposition/resuspension processes to/from surfaces exposed to the gas phase, $BAS1_i$ is used with dry atmospheric conditions and $BAS2_i$ with wet conditions, i.e. with wall condensation. For all other reactions in the gas phase and all processes and reactions in the water phase $BAS1_i$ values are used. In Chapter 4, Table 4-1, the values for $BAS1_i$ and $BAS2_i$ as well as the corresponding activation energies $EAKT1_i$ and $EAKT2_i$ are summarized.

The hydrogen ion concentration $[H^+]$ is given as boundary condition calculated from the input pH value. The implementation of a model which calculates the pH as function of temperature and chemical composition of the sump is planned.

3.2 Water phase reactions

3.2.1 Inorganic iodine hydrolysis reactions

I_2 dissolved in water is subject to hydrolysis, producing a large spectrum of intermediate and stable iodine species. Amongst these, the three more stable iodine species hypoiodous acid (HOI, iodine oxidation state +1), iodide (I^-, iodine oxidation state -1) and iodate (IO_3^-, iodine oxidation state +5) are modelled in two empirical hydrolysis steps taken from /BEL 82/:

- step 1: fast formation of HOI and I^-
- step 2: slow formation of IO_3^-

This empirical two-step concept avoids the mechanistic modelling of numerous short-lived iodine species in several chemical reactions. Thus CPU time in plant applications can be significantly reduced. The disadvantage is a less comprehensive modelling of individual laboratory tests.

Hydrolysis step 1

$$I_2 + H_2O \underset{k(12)}{\overset{k(11)}{\rightleftharpoons}} HOI + I^- + H^+$$

$$\begin{aligned} d\,I2/dt &= -k(11) \cdot I2 \\ &\quad + k(12) \cdot IMINUS \cdot HOI \cdot HPLUS \end{aligned}$$

$$\begin{aligned} d\,HOI/dt &= +k(11) \cdot I2 \\ &\quad - k(12) \cdot IMINUS \cdot HOI \cdot HPLUS \end{aligned}$$

$$\begin{aligned} d\,IMINUS/dt &= +k(11) \cdot I2 \\ &\quad - k(12) \cdot IMINUS \cdot HOI \cdot HPLUS \end{aligned}$$

The rate constant k(11) is calculated from the BAS and EAKT values. The H^+ concentration is given by the pH of the sump:

$$HPLUS = 10^{-pH}.$$

The rate constant k(12) is calculated from the equilibrium constant KHIO and the rate constant k(11):

$$k(12) = k(11) / KHIO$$

The equilibrium constant KHIO is defined by the equilibrium concentrations of the involved iodine species:

$$KHIO = (IMINUS_{EQ} \cdot HOI_{EQ} \cdot HPLUS_{EQ}) / I2_{EQ}$$

KHIO is calculated as function of the sump temperature /LEM 81/:

$$KHIO = 10^{\left(-\frac{5.634 \cdot 10^5}{TKSUMP^2} + \frac{5.757 \cdot 10^2}{TKSUMP} - 7.893\right)}$$

TKSUMP sump temperature in K

Hydrolysis step 2

$$3\ HOI \underset{k(15)}{\overset{k(13)}{\rightleftharpoons}} IO_3^- + 2\ I^- + 3\ H^+$$

The strongly pH-dependent reverse reaction is the so-called Dushman reaction, as taken from /FUR 72/.

$$d\ IO3MIN/\ dt = + k(13) \cdot HOI^2 \cdot 1/3 - k(15) \cdot IO3MIN \cdot IMINUS^{N15} \cdot HPLUS^2$$

$$d\ IMINUS/\ dt = + k(13) \cdot HOI^2 \cdot 2/3 - k(15) \cdot IO3MIN \cdot IMINUS^{N15} \cdot HPLUS^2 \cdot 2$$

$$d\ HOI/\ dt = - k(13) \cdot HOI^2 + k(15) \cdot IO3MIN \cdot IMINUS^{N15} \cdot HPLUS^2 \cdot 3$$

The rate constant k(13) is calculated as function of pH and temperature according to the "Toth model" /TOT 84/:

pH = 6: AK6 = - 11.52E+3/TKSUMP + 34.90

pH = 7: AK7 = - 8.90E+3/TKSUMP + 30.45

pH = 8: AK8 = - 5.79E+3/TKSUMP + 23.34

pH = 9: AK9 = - 4.47E+3/TKSUMP + 20.40

pH = 10: AK10 = - 3.42E+3/TKSUMP + 16.81

pH < 7: ALOGK = AK6 + (AK7 - AK6) * pH – 6.0)

7 < pH < 8: ALOGK = AK7 + (AK8 - AK7) * (pH – 7.0)

8 < pH < 9: ALOGK = AK8 + (AK9 - AK8) * (pH – 8.0)

pH > 9: ALOGK = AK9 + (AK10 - AK9) * (pH – 9.0)

k(13) = exp(ALOGK)

As temperature dependency is already included in the Toth model, no additional Arrhenius formalism is applied to k(13).

The value of parameter N15 is set to 1.0 in AIM-3.

Rate constants k(12) and k(13)

As the rate constants k(12) and k(13) and their temperature dependencies are calculated by the code, their BAS and EAKT values are set to zero in the input file. Changing these values in the input file has no effect on the calculation.

Oxidation of iodide by dissolved oxygen

Iodide in aqueous solutions with dissolved air from the atmosphere above the sump is slowly oxidized, producing aqueous I_2. The model is taken from /GÜN 92/:

$$\mathbf{2\ I^- + 1/2\ O_2 + 2\ H^+} \xrightarrow{k(16)} \mathbf{I_2 + H_2O}$$

$$d\ I2\ /dt = + k(16) \cdot IMINUS \cdot HPLUS$$

$$d\ IMINUS\ /dt = - k(16) \cdot IMINUS \cdot HPLUS \cdot 2$$

BAS(16) = 1.0E-7 l/(mol·s), EAKT(16) = 4.6E+4 J/mol

There is neither an explicite modelling of oxygen dissolution from air, nor is the dissolved oxygen modelled explicitly. The presence of oxygen is implicitly considered in the rate constant k(16). Due to the lower importance of reaction no. 16 in plant applications the model uncertainties are less significant. In conditions where the aqueous oxygen is depleted, e.g. in boiling sumps, the reaction is switched off.

3.2.2 Inorganic iodine radiolysis reactions

Reactive intermediate species that react further with iodine species are formed by radiolysis of water. This very complex process is simplified in the following chemical equations /GÜN 92/.

Radiolytic I_2 formation from I^-

Under accident conditions this reaction is the main source for I_2 in the sump and consequently for I_2 in the gas phase.

$$\mathbf{2\ I^- + \gamma} \underset{k(21)}{\overset{k(20)}{\rightleftarrows}} \mathbf{I_2 + 2\ e^-}$$

The I_2 concentration is modelled by

d I2 /dt = + k(20) · IMINUS · $HPLUS^{N20}$ · D_S
- k(21) I2

d IMINUS /dt = - 2 · d I2 /dt

D_S dose rate in the sump (kGy/h)

N20 exponent describing the pH dependency (= 0.2)

As a result of the International Standard Problem ISP-41 Follow up / Phase 2, the parameters N20 and N29 (IO_3^--decomposition, see below) were reduced from 0.5 to 0.2 because of a systematic overestimation of the I_2(g) concentration. These new values describe the analyzed ISP-41 tests significantly better. The rate constants k(20) and k(29) were reduced accordingly /WEB 05/.

In the model the reverse reaction rate (no. 21) cannot become faster than the forward reaction rate (no. 20). This is to exclude a wrong I_2 destruction and iodide production through reaction no. 21 in the absence of radiation.

Radiolytic formation of I_2 from IO_3^-

$$\mathbf{2\ IO_3^- + \gamma} \underset{k(34)}{\overset{k(29)}{\rightleftarrows}} \mathbf{I_2}$$

d I2 /dt = + k(29) · IO3MIN · $HPLUS^{N29}$ · D_S
- k(34) · I2

d IO3MIN /dt = - 2 d I2 /dt

N29 exponent describing the pH dependency (= 0.2)

In the model the reverse reaction rate (no. 34) cannot become faster than the forward reaction rate (no. 29). This is to exclude a wrong I_2 production and iodate destruction through reaction 34 in the absence of radiation.

Remarks on the hydrolysis and radiolysis models

The experimental data from the EPICUR facility tests S1-3, S1-4 and S1-5 on inorganic iodide radiolysis and hydrolysis at high temperatures (80°C, 120°C), high dose rates (3.6 - 3.8 kGy/h), and pH 5 were reasonably well reproduced by the sum of the above modelled hydrolysis and inorganic iodine radiolysis steps /FUN 08/. However, the volatile I_2 resulting in the pH 7 test S1-11 was overestimated by a factor of 10 in this validation work. This work also showed that the discrepancy at pH 7 could be removed by adjusting model parameters of reaction 20. However, the above model obtained during the ISP-41 project /WEB 05/ will be used as long as there are no additional data analyses at high pH.

3.2.3 Silver / iodine reactions

Phenomena

Silver (Ag) aerosol particles from degraded control rods are transported by settling and wash-down processes into the sump. The dissolved iodine deposits on the surface of the Ag particles where it forms poorly soluble silver iodide (AgI). In reactor applications silver represents an efficient iodine sink.

The model taken from /DIC 99/ is based on experimental studies perfomed at AEA Technology using silver sheets /DIC 99/ and at Siemens using silver powder /FUN 96a/. Following these studies AgI formation from I_2 and from I^- is distinguished. In AIM it is assumed that the silver particles are always suspended homogeneously within the sump. However, this is not realistic, because the heavy silver particles will settle quickly. The reduced reactivity of silver particles mixed to the sludge at the sump bottom is not considered in the model. This effect is important as the analysis of the Phebus FPT1 test demonstrates /WEB 08/.

Only with sump boiling and sump flashing a carry-over of AgI particles into the gas phase is possible in AIM (s. wet resuspension in Chapters 3.4 and 5).

Model

Four major processes are modelled in AIM.

Process 1: Aqueous I_2 reacts with Ag according to:

$$\mathbf{I_2 + 2\ Ag} \xrightarrow{k(28)} \mathbf{2\ AgI}$$

d I2 /dt = - 1/(1/k_W+1/(k(28)·AG))·I2·AG·S_{AG}·MAG·1000

= + 1/2 d AG /dt

= - 1/2 d AGI /dt

AGI	concentration of AgI in mol/l
AG	concentration of Ag in mol/l
I2	concentration of I_2 in mol/l
k_W	aqueous mass transfer constant in m/s
k(28)	BAS(28) = 0.2 m·l·mol^{-1}·s^{-1}, EAKT(28) = 0
S_{AG}	specific area of Ag particles = surface area of all Ag particles over the Ag mass, m^2/g, recommended for containment: 6.0E-3 m^2/g (derived following Phebus-FPT1 analyses /WEB 08/)
MAG	atomic weight of Ag, 107.87 g/mol
1000	dimension factor in l·m^{-3}

The pH value is no parameter because no pH effect on the reactivity of the Ag surface with respect to I_2 was observed at pH 3 and pH 4.6. AgI formation is not dependent on temperature in the experimentally studied range from 20°C to 160°C.

Process 2: The Ag surface is at least partially oxidised by dissolved oxygen. This reaction is a prerequisite for the reaction of I^- with Ag particles:

$$\mathbf{Ag + O_2} \xrightarrow{k(73)} \mathbf{AgO_x}$$

d AGOX /dt = + k(73)·AG·S_{AG}·MAG

= - d AG /dt

AG	concentration of Ag in mol/l
AGOX	concentration of oxidized Ag in mol/l
k(73)	BAS(73) = 8.7E-9 mol/m^{-2}·s^{-1}

Temperature and pH dependency of k(73) is modelled according to:

K7390 = exp(-0.570735·pH - 14.9198)

EAKT(73) = R·ln(BAS(73)/K7390)/(1./363.15-1./298.15), J/mol

K(73) = BAS(73) exp((EAKT(73)/R)·(1/298.15-1/TKSUMP))

TKSUMP	sump temperature, K
R	gas constant 8.3144 J/(mol·K)

AgO_x formation is automatically switched off

- during boiling sump conditions because of little oxygen in the sump,
- at pH > 7 because no AgO_x formation was observed experimentally in basic water.

The oxygen O_2 is not modelled.

Process 3: AgI is produced from a reaction between I^- and AgO_x:

$$\mathbf{AgO_x + I^- + 2\ H^+} \xrightarrow{k(56)} \mathbf{AgI + H_2O}$$

d AGI/dt = +1/(1/k_W+1/(k(56)·AGOX))·IMINUS·AGOX·S_{AG}·MAG·1000

= - d IMINUS /dt

= - d AGOX /dt

k(56)	reaction rate, 2 m·l·mol^{-1}·s^{-1} at 25°C (=BAS(56); EAKT(56)=0)
	IMINUS conc. of I^- in mol/l

The term AGOX·S_{AG}·MAG describes the total surface area of the oxidized silver related to the sump volume.

Process 4: AgI destruction by radiolysis:

$$\mathbf{2\ AgI\ +\ \gamma} \underset{k(27)}{\overset{k(26)}{\rightleftarrows}} \mathbf{I_2\ +\ 2\ Ag}$$

d I2 /dt = + k(26) · AGI · D_S

- k(27) · I2

d AG /dt = - d AGI /dt = 2 d I2 /dt

Reactions 26 and 27 are currently not considered in AIM and the respective default rate constants are set to zero. Future model developments are conceivable, based e.g. upon more recent studies at PSI and taking into account the limited solubility of AgI.

In the model the reverse reaction rate (no. 27) cannot become faster than the forward reaction rate (no. 26). This is to exclude a wrong I_2 destruction and AgI production through reaction no. 27 in the absence of radiation.

Ag surface area

The surface of all Ag particles is calculated from the Ag mass concentration and the specific Ag surface area assuming that the Ag particles are suspended homogeneously in the sump. The aqueous Ag concentration is given in the AIM input or it is calculated by the aerosol model in COCOSYS. In the first case the fraction of Ag reaching the sump needs to be checked for plausibility by the user since the current-down model is uncertain.

The recommended value for the specific Ag surface in the sump of a containment is S_{AG} = 6E-3 m^2/g, as derived from a PHEBUS-FPT1 analysis /WEB 08/. Analyses of laboratory experiments on the Ag/iodine reaction using defined Ag powder may require much larger S_{AG} values. In /FUN 96a/ a measured value of 0.2 m^2/g was used for evaluation of the experiments, being consistent with the used pure, spherical Ag particles with diameters in the range 2 - 3.5 µm which were homogeneously distributed in the aqueous phase.

Still open questions on the Ag/iodine model

- The specific Ag surface S_{AG} is constant with time in the model. Agglomeration which would decrease S_{AG} is not considered, as a corresponding Ag agglomeration model is not available.
- In realistic sumps, most of the silver particles should rapidly be sedimented at the bottom. Instead, the model assumes the sump to be a mixed Ag suspension. The transport of iodine through the aqueous phase down to Ag deposits is not modelled, as no direct experimental information is at hand.
- Another effect of realistic sumps is the mixing of Ag into a sludge formed by different materials. This could reduce the rates of the Ag/iodine reactions due to a restricted contact of iodine with the Ag surface. No experimental information is available yet.

The effects of agglomeration, sedimentation, and sludge formation of Ag particles might implicitly be considered in the above mentioned default value S_{AG} = 6E-3 m^2/g derived from a PHEBUS-FPT1 analysis /WEB 08/. However, this could be a specific result of the FPT1 test and is not necessarily valid with other boundary conditions.

The default values of the initial AgOx fraction of 10 % is only indirectly deduced from code interpretations of the PHEBUS tests FPT0 and FPT1 /GIR 04/.

3.2.4 Organic iodine reactions in the homogeneous phase

Formation of organic iodide in the sump

In containment sumps organic iodide is formed from reactions of iodine with various organic compounds prevailing like oil, organic solvents or destruction products leached from painted surfaces, and cable insulation.

AIM-3 treats the formation of organic iodides (CH_3I) in the homogeneous water phase as reactions of the iodine species I_2 (w) and HOI (w) with reactive organic compounds called CH_3 (w):

$$\mathbf{I_2\ (w)\ +\ 2\ CH_3\ (w)} \underset{k(23)}{\overset{k(22)}{\rightleftarrows}} \mathbf{2\ CH_3I\ (w)}$$

$$\mathbf{HOI\ (w)\ +\ CH_3\ (w)} \underset{k(41)}{\overset{k(40)}{\rightleftarrows}} \mathbf{CH_3I\ (w)\ +\ OH^-\ (w)}$$

$$\begin{aligned}
\text{d CH3I /dt} &= + k(22) \cdot I2 \cdot CH3 \cdot 2 \\
&\quad - k(23) \cdot CH3I \cdot 2 \\
&\quad + k(40) \cdot HOI \cdot CH3 \\
&\quad - k(41) \cdot CH3I \\
\text{d I2 /dt} &= - k(22) \cdot I2 \cdot CH3 \\
&\quad + k(23) \cdot CH3I \\
\text{d HOI /dt} &= - k(40) \cdot HOI \cdot CH3 \\
&\quad + k(41) \cdot CH3I \\
\text{d CH3 /dt} &= - \text{d CH3I / dt}
\end{aligned}$$

The OH^- concentration is not modelled. The default rate constants of the three back reactions are set to zero in AIM-3, i.e. k(23) = 0 and k(41) = 0.

The model was taken from IMPAIR-3. The original IMPAIR-3 model was adapted to the ACE/RTF tests /GÜN 92/. The rate constants (Table 4-1) are not explicitly validated.

Destruction of organic iodide in the sump by water and hydroxide

The empirical model includes two parallel pathways to hydrolyse CH_3I (w), the hydrolysis by H_2O and that by OH^-, both producing aqueous I^-:

$$\mathbf{CH_3I\ (w) + H_2O} \underset{k(31)}{\overset{k(30)}{\rightleftarrows}} \mathbf{I^-\ (w) + CH_3 + H^+}$$

$$\mathbf{CH_3I\ (w) + OH^-} \underset{k(33)}{\overset{k(32)}{\rightleftarrows}} \mathbf{I^-\ (w) + CH_3}$$

d CH3I /dt = - k(30) · CH3I
- k(32) · CH3I ·1E-14/HPLUS
+ k(31) · IMINUS · HPLUS · CH3
+ k(33) · IMINUS · CH3

d IMINUS /dt = + k(30) · CH3I
+ k(32) · CH3I · 1E-14/HPLUS
- k(31) · IMINUS · HPLUS · CH3
- k(33) · IMINUS · CH3

d CH3 /dt = - d CH3I /dt

Radiolytic destruction of organic iodide in the sump

The radiolytic destruction of CH_3I (w) producing aqueous I_2 is modelled empirically according to:

$$\mathbf{CH_3I\ (w)} + \gamma \underset{k(25)}{\overset{k(24)}{\rightleftarrows}} \mathbf{I_2\ (w) + CH_3\ (w)}$$

d CH3I /dt = - k(24) · CH3I · D_S · 2
+ k(25) · I2 · CH3 · 2

$$d\,I2/dt = +k(24) \cdot CH3I \cdot D_S - k(25) \cdot I2 \cdot CH3$$

$$d\,CH3/dt = -d\,CH3I/dt$$

The defaults of the three back reactions are set to zero in AIM-3, i.e. k(31) = 0, k(33) = 0 and k(25) = 0.

This model is also taken from IMPAIR-3. The IMPAIR-3 model was adapted to integral ACE/RTF tests /GÜN 92/. The rate constants (Table 4-1) are not explicitly validated.

In the model the reverse reaction rate (no. 25) cannot become faster than the forward reaction rate (no. 24). This is to exclude a wrong I_2 destruction and CH_3I production at low or zero dose rates.

Organic residues

The species CH_3 (w), i.e. organic residues, is a modelled species in AIM-3 and requires the assignment of an initial concentration. Due to considerations in /BEA 87/ and measurements in primary systems /HOF 95/, organics concentrations in the sump could be in the order of 1E-5 mol/l. This concentration is used as default value of CH_3 (w) in the input file. It varies during AIM calculations by various reactions and mass transfer between water and gaseous phases.

3.2.5 Iodine reactions with immersed painted surfaces

Aqueous iodine is deposited onto immersed painted surfaces and a part is resuspended back into the sump water. Iodine deposited onto paint can chemically react with the paint to non-soluble iodine.

The model considers:

- deposition of the aqueous species I_2 and I^-
- resuspension of I_2, I^- and CH_3I back into water from **I_2 loaded** paint
- resuspension of I^- and CH_3I back into water from **I^- loaded** paint

Deposition and resuspension of molecular iodine

I_2 is deposited onto paint and resuspended from paint as I_2 according to:

$$\mathbf{I_2(w)} \underset{k(38)}{\overset{k(17)}{\rightleftarrows}} \mathbf{I_2(dep,p,w)}$$

$$\frac{dI2}{dt} = -k(17) \cdot I_2 \cdot S/V + k(38) \cdot DEPWP \cdot S/(V \cdot 1000)$$

$$\frac{dDEPWP}{dt} = +k(17) \cdot I_2 \cdot 1000 - k(38) \cdot DEPWP$$

BAS(17) = 2E-6 m/s, EAKT = 9.59E+3 J/mol

$T_{sump} \leq 90\ ^0C$: BAS1(38) = 4.16E-9 s^{-1}, EAKT1 = 8.55E+4 J/mol

$T_{sump} > 90\ ^0C$: k(38) = 2E-6 s^{-1}

At low temperatures (≤ 90 ^{0}C) the resuspension rate k(38) increases with temperature according to the Arrhenius relation. At high temperatures the rate is assumed to be constant.

Caution: k(38) is stored in the code separately from the BAS1 and BAS2 values and cannot be changed via input.

Resuspension of iodide after loading with molecular iodine

Resuspension of I^- from paint after loading with I_2 is modelled as:

$$\mathbf{I_2\ (dep,p,w)} \overset{k(69)}{\rightarrow} \mathbf{2\ I^-(w)}$$

$$\frac{dDEPWP}{dt} = -k(69) \cdot DEPWP$$

$$\frac{dIMINUS}{dt} = +k(69) \cdot DEPWP \cdot S/(V \cdot 1000) \cdot 2$$

BAS(69) = 8.58E-7 s^{-1}, EAKT(69) = 5.1E+4 J/mol

Experimental study

The I_2/paint model is based upon an experimental parameter study with temperatures between 25° C and 140° C /HEL 96/. In tests with I_2, pH values were generally at about 2. The low value was chosen in order to avoid I_2 hydrolysis. In tests with I^-, pH values

were about 2 or about 5. The Epoxy paint coupons were aged by storage at room temperature for at least 100 days or artificially aged up to about 6 years.

Given the new insights into chemisorption in the I^-/paint system described below /LAN 08b/, it seems to be necessary to re-assess the I_2/paint model.

Deposition and resuspension of iodide

Deposition of aqueous I^- onto immersed paint, resuspension of I^- from paint and fixation of iodide in a non-soluble form is modelled based upon recent laboratory tests performed within the German national THAI-3 project and according to /LAN 08b/:

$$\mathbf{I^-(w)} \underset{k(19)}{\overset{k(37)}{\rightleftarrows}} \mathbf{I^-(dep,p,w)} \underset{k(80)}{\overset{k(79)}{\rightleftarrows}} \mathbf{Ichs(dep,p,w)}$$

$$\begin{aligned}
\text{d IMINUS /dt} &= -\,k(37)\cdot \text{IMINUS}\cdot S/V \\
&\quad +\,k(19)\cdot \text{DEPWI}\cdot S/(V\cdot 1000) \\
\text{d DEPWI /dt} &= +\,k(37)\cdot \text{IMINUS}\cdot 1000 \\
&\quad -\,k(19)\cdot \text{DEPWI} \\
&\quad -\,k(79)\cdot \text{DEPWI} \\
&\quad +\,k(80)\cdot \text{DEPW_ICHS} \\
\text{d DEPW_ICHS /dt} &= +\,k(79)\cdot \text{DEPWI} \\
&\quad -\,k(80)\cdot \text{DEPW_ICHS}
\end{aligned}$$

The correlations for reactions no. 19 and 37 are truncated at AGE = 5 years, i.e. between AGE = 0 (totally fresh paint) and AGE = 5 the reaction constants and activation energies are kept konstant at the values for AGE = 5.

For $0 \le$ AGE $\le$ 5 years:

$BAS(19) = 1.3\ E\text{-}5 \cdot 5$

$EAKT(19) = -\ 2.15\ E3 \cdot 5 + 1.06\ E4 + 4.91\ E6 \cdot [H^+]$

$BAS(37) = (-\ 1.21\ E\text{-}9 + 2.53\ E\text{-}7 \cdot [H^+]) \cdot 5 + 4.24\ E\text{-}8 - 7.84\ E\text{-}6 \cdot [H^+]$

$EAKT(37) = (-\ 2.25\ E3 + 2.04\ E5 \cdot [H^+]) \cdot 5 + 6.16\ E4 + 6.92\ E6 \cdot [H^+]$

and for AGE > 5 years:

BAS(19) = 1.3 E-5 · AGE

EAKT(19) = - 2.15 E3 · AGE + 1.06 E4 + 4.91 E6 · $[H^+]$

BAS(37) = (- 1.21 E-9 + 2.53 E-7 · $[H^+]$) · AGE + 4.24 E-8 – 7.84 E-6 · $[H^+]$

EAKT(37) = (- 2.25 E3 + 2.04 E5 · $[H^+]$) · AGE + 6.16 E4 + 6.92 E6 · $[H^+]$

BAS(79) = 5E-6

EAKT(79) = 0

BAS(80) = 0

EAKT(80) = 0

BAS(37): dimension is m/s

BAS(19), BAS(79), BAS(80): dimension is 1/s

AGE: Age of paint in years

AGE = 30 years is recommended if no additional information is available or if a plant calculation with conservative results shall be made. With a high paint age the iodine trapping on the sump walls is small and hence the gaseous iodine concentration in the containment rises.

Experimental study

In the laboratory tests /LAN 08b/ temperatures between 25°C and 90°C, and as well as pH values of 2.5, 5 and 7 were considered. Epoxy paint as used in many German NPPs was artificially aged to 5 and 30 years. Reproduction tests were carried out successfully and the data are reliable /LAN 08b/. No measurements are available for a paint age under 5 years and that is why the correlations no. 9 and 37 are truncated below this age. For pH values much larger than 7 the rates are rather uncertain because the database is scarce already at pH 7. The measured iodine deposition decreases with increasing age and pH, but increases with temperature.

Additional experimental data on the deposition and resuspension of iodide on and from immersed paint are expected from the current OECD-BIP project.

The model parameter AGE is limited in AIM-3 to values larger than or equal to 5 years, even if the user input would be lower. This limitation excludes non-allowed extrapolations to lower ages than studied in the experimental program and prevents calculations using unrealistically depleted iodide resuspension from paint through reaction 19 and thus producing unrealistic high iodide depositions on immersed paint.

The calculated activation energies of reactions 19 and 37 can assume negative values. According to standard textbooks on kinetics, negative apparent activation energies can occur e.g. for complex mechanisms, which consist of the sequence of establishing an equilibrium in a first step and a follow-up reaction as a second step. Another explanation of negative activation energy could be that the Arrhenius concept is not applicable in this case, and that the derived EAKT values just represent empirical model parameters. In the latter case, modelling of EAKT as function of pH would not be contradictory to the Arrhenius concept.

Release of CH_3I from iodine-loaded paint

The release of organic iodide from iodine-loaded painted surfaces in the aqueous phase is modelled analogously to the modelling for the gas phase, see Ch. 3.3.3.

Thermal CH_3I release

I_2 (dep,p,w) $\xrightarrow{k(39)}$ **2 CH_3I (w)**

I^- (dep,p,w) $\xrightarrow{k(39)}$ **CH_3I (w)**

I_{chs} (dep,p,w) $\xrightarrow{k(39)}$ **CH_3I (w)**

$$\frac{d\,CH3I}{dt} = + k(39)\, DEP^g \cdot S/(V \cdot 1000)$$

$$DEP = 2 \cdot DEPWP + DEPWI + DEPW\_ICHS$$

$$\frac{d\,DEPWP}{dt} = - k(39) \cdot 0.5 \cdot (2 \cdot DEPWP)^g$$

$$\frac{d\,DEPWI}{dt} = - k(39) \cdot DEPWI^g$$

$$\frac{d\,DEPW\_ICHS}{dt} = - k(39) \cdot DEPW\_ICHS^g$$

BAS(39) = 1.5E-12 $s^{-1}(m^2/mol)^{g-1}$, EAKT(39) = 7.84E+4 J/mol

With the empirical exponent g = 0.5.

In order to increase the numerical stability at very small reaction rates the rate no. 39 is limited by

d CH3I /dt ≥ DEPWP · 0.1

Radiation-induced CH_3I release

I_2 (dep,p,w) + γ $\xrightarrow{k(18)}$ **2 CH_3I (w)**

I^- (dep,p,w) + γ $\xrightarrow{k(18)}$ **CH_3I (w)**

I_{chs} (dep,p,w) + γ $\xrightarrow{k(18)}$ **CH_3I (w)**

$$\frac{d\,CH3I}{dt} = + k(18)\cdot DEP^{h} \cdot D_S \cdot S/(V\cdot 1000)$$

$$DEP = 2\cdot DEPWP + DEPWI + DEPW\_ICHS$$

$$\frac{d\,DEPWP}{dt} = - k(18) \cdot 0.5 \cdot (2\cdot DEPWP)^{h} \cdot D_S$$

$$\frac{d\,DEPWI}{dt} = - k(18) \cdot DEPWI^{h} \cdot D_S$$

$$\frac{d\,DEPW\_ICHS}{dt} = - k(18) \cdot DEPW\_ICHS^{h} \cdot D_S$$

BAS(18) = 3.6E-9 $s^{-1}(kGy/h)^{-1}(m^2/mol)^{h-1}$, EAKT(18) = 1.97E+4 J/mol

With the empirical exponent h = 0.426.

In order to increase the numerical stability at very small reaction rates rate 18 is limited by

d CH3I /dt ≥ DEPWP · 0.1

Model restriction

The model of thermal and radiation-induced RI release from immersed iodine-loaded paint was adapted from the gas phase model (Chapter 3.3.3). No separate validation has been performed, and the modelling uncertainty is considered to be large. Since in a severe accident the RI is expected to be produced mostly on the painted surfaces exposed to the gas phase, this uncertainty of the aqueous phase model will have little influence on the overall RI prediction in the containment. The values of the rate constants BAS(39) and BAS(18) were taken from the corresponding gas phase model.

3.2.6 Iodine reaction with immersed steel surface

Aqueous I_2 reacts with immersed steel surfaces to produce metal iodides. As these metal iodides are readily soluble in water, no resident iodine loading on the surface is modelled. The model therefore considers the conversion of aqueous I_2 into aqueous I^- by the reaction at the steel surface according to /FUN 96b/, partially revised /WEB 09/:

I_2 (w) + steel (w) $\overset{k(55)}{\rightarrow}$ **2 I^- (w)**

d I2 /dt = - k(55) · I2 · S/V
= - d IMINUS /dt · 1/2

BAS(55) = 1.25E-7 m/s

EAKT (55) = 8.08E+4 J/mol

Reaction constant k(55)

Analyses of the THAI test Iod-9 /WEB 09/ reveal that the conversion of I_2 into I^- at about 60 °C is much faster (5E-6 m/s) than the original rate constant (9.2E-8 m/s) /FUN 96b/ from laboratory tests. No explanation is at hand for this discrepancy. The above default of BAS(55) value is based upon the THAI test value of 5E-6 m/s, but the activation energy measured in the laboratory tests is retained. In the reactor case, due to the typically small immersed steel surface areas, this model uncertainty should be of lower importance.

3.2.7 Iodine reactions with immersed, bare concrete surfaces

The interaction of aqueous iodine with immersed, bare concrete surfaces is modelled in a very simplified way by the deposition of aqueous I_2 on concrete and the resuspension from the immersed concrete in iodide form:

I_2 (w) $\overset{k(57)}{\rightarrow}$ **I_2 (dep,c,w)**

I_2 (dep,c,w) $\overset{k(58)}{\rightarrow}$ **2 I^- (w)**

d I2 /dt = - k(57) · I2 · S/V

d IMINUS /dt = + k(58) · DEPWC · S/(V·1000) · 2

$$d\,DEPWC/dt = +k(57) \cdot I2 \cdot 1000 - k(58) \cdot DEPWC$$

BAS(57) = 2.0E-5 m/s, EAKT(57) = 0

BAS(58) = 1.0E-2 1/s, EAKT(58) = 0

The rate constants are assumed values and not validated. The whole model is retained from IMPAIR /GÜN 92/, where it had been integrated provisionally. No plans exist to remove the model uncertainty as bare concrete surfaces are of little interest in most plant applications.

3.3 Gas phase reactions

3.3.1 Iodine / ozone reaction

In irradiated air/steam atmospheres I_2 (g) is oxidized by radiolysis products, e.g. ozone (O_3), into iodine oxides (IO_x), where x represents several stoichiometries /VIK 85/. In typical containment conditions with a high humidity, condensate on the walls and sometimes fog, IO_x will quickly be converted into iodate (IO_3^-). In the AIM model this iodine oxide/iodate conversion is not treated explicitly. The I_2/O_3 reaction directly leads to gasborne iodate in aerosol form (gas-to-particle conversion). The I_2/O_3 reaction converts a volatile iodine species into a non-volatile but still mobile iodine aerosol. This fact together with the fast conversion makes the reaction important for source term considerations.

By use of measurement experience from THAI /FUN 09a and 09b/ a re-evaluation of Maypack filters from PHEBUS FP-Tests delivered a clear evidence of the occurrence of IO_x aerosols under severe accident conditions /GIR 08/.

Model

The empirical model is essentially taken from irradiated experiments respectively their interpretation given in /FUN 99/. The earlier Canadian experimental and modelling work in non-irradiated conditions /VIK 85/ is also considered.

$$I_2\,(g) + O_3\,(g) \underset{k(2)}{\overset{k(1)}{\rightleftarrows}} 2\ IO_3^-\,(g)$$

Ozone representing all oxidizing radiolysis products is produced by radiolysis of the air / steam atmosphere:

$$\text{air / steam atmosphere} + \gamma \underset{k(72)}{\overset{k(71)}{\rightleftarrows}} O_3\,(g)$$

It is noted that the apparent reverse reaction 2 produces I_2 (g) but no O_3 (g) in the model.

The build-up of ozone is limited by its natural destruction, which is a consequence of its high chemical reactivity. Four different destruction processes are modelled. Reaction 72 and 78 concern the radiation-induced and the thermal destruction of O_3, and the reactions 82 and 83 describe the decomposition of O_3 by painted and steel surfaces /FUN 99/. The modelled kinetic equations are:

$$\begin{aligned}
\frac{dO3G}{dt} &= +k(71)\cdot D_G && \text{production of } O_3\\
&\quad -k(1)\cdot STOFAC\cdot O3G\cdot I2G && \text{formation of } IO_x\\
&\quad -f_{72}\cdot k(72)\cdot O3G\cdot D_G && \text{radiation-induced decomp. of } O_3\\
&\quad -k(82)\cdot S_{PAINT,G}/V_G\cdot O3G && \text{decomposition of } O_3 \text{ by paint}\\
&\quad -k(83)\cdot S_{STEEL,G}/V_G\cdot O3G && \text{decomposition of } O_3 \text{ by steel}\\
&\quad -f_{78}\cdot k(78)\cdot O3G && \text{thermal decomposition of } O_3
\end{aligned}$$

$$\begin{aligned}
\frac{dI2G}{dt} &= -k(1)\cdot O3G\cdot I2G\\
&\quad +k(2)\cdot IO3MING\cdot D_G/2
\end{aligned}$$

$$\begin{aligned}
\frac{dIO3MING}{dt} &= +k(1)\cdot O3G\cdot I2G\\
&\quad -k(2)\cdot IO3MING\cdot D_G/2
\end{aligned}$$

with

$$f_{72} = \exp(6.957\,(\rho_{ST} - 1))$$

$f_{78} = \exp(8.685\ (\rho_{ST} - 1))$

D_G dose rate in the gas phase (kGy/h)

STOFAC stoichiometric factor, = 3.9 /VIK 85/

$S_{PAINT,G}$ painted surface in gas phase (m²)

$S_{STEEL,G}$ steel surface in gas phase (m²)

ρ_{ST} steam density (g/l).

The dimensionless parameters f_{72} and f_{78} correlate the O_3 destruction rates with the steam content in the atmosphere.

The rate constants at 25°C and the activation energies are:

BAS(1) = 2400 l $mol^{-1}s^{-1}$, EAKT(1) = 25.0 ± 1.2 kJ mol^{-1}

BAS(71) = $4.7 \cdot 10^{-11}$ mol/l s^{-1} $(kGy/h)^{-1}$, EAKT(71)= 0

BAS(72) = $4.3 \cdot 10^{-2}$ $(s \cdot kGy/h)^{-1}$, EAKT(72) = 11.2 kJ/mol

BAS(82) = $1.27 \cdot 10^{-5}$ ms^{-1}, EAKT(82) = 58.3 kJ mol^{-1}

BAS(83) = $1.46 \cdot 10^{-5}$ ms^{-1}, EAKT(83) = 56.2 kJ mol^{-1}

BAS(78) = $3 \cdot 10^{-4}$ s^{-1}, EAKT(78) = 58.1 kJ/mol,

The rate constants k(72) and k(78), as well as the parameters f_{72} and f_{78} describing the dependency of O_3 destruction as function of steam concentration, were obtained from an unpublished AREVA analysis of O_3 destruction data measured in /FUN 99, FUN 06, FUN 09/. Corresponding data of the PARIS project /LAN 05/ are consistent with this model.

These rate constants are valid for the following boundary conditions:

Temperature: 20 - 130°C

Dose rate: 1.5 – 20 kGy/h

Atmosphere: moist and dry air

The rate constant k(1) is taken from the original Vikis model /VIK 85/, and it is consistent with the data in /FUN 99/.

The rate constant k(71) is based upon experimental data and their analyses as taken from /FUN 99/. Within the experimental uncertainties, the rate constant k(71) is considered to be independent of steam concentration. The PARIS project tests in air/steam mixtures revealed very similar production rates /BOS 08/. The original value k(71)= $5.8 \cdot 10^{-11}$ mol/l s^{-1} $(kGy/h)^{-1}$ was slightly reduced according to the experience made in ASTEC calculations on PHEBUS FPT1. The original rate constants k(82) and k(83) at 25 °C from /DIC 03/ were replaced by much higher values given in /BOS 09/. The activation energies are still those from /DIC 03/. The modified O_3 model was validated by COCOSYS/AIM-3 calculations on PHEBUS FPT1.

The aerosol behaviour modelling of the IO_3^- aerosol is described in the Chapters 3.4.3 and 5.3.

3.3.2 Organic iodide destruction in the gas phase

Organic iodide in the homogeneous gas phase is decomposed in the presence of a radiation field. The model stems from /TAN 70/ and includes I_2(g) as the resulting reaction product:

$$\mathbf{CH_3I\ (g)\ +\ \gamma\ \underset{k(67)}{\overset{k(65)}{\rightleftarrows}}\ 1/2\ I_2(g)\ +\ CH_3(g)}$$

The reverse reaction 67 is modelled formally, but switched off by setting the default rate constant to zero.

$$\begin{aligned} \text{d CH3IG /dt} &= -\ k(65) \cdot \text{CH3IG} \cdot D_G \\ &= -\ \text{d I2G /dt} \cdot 2 \\ &= -\ \text{d CH3G /dt} \end{aligned}$$

BAS(65) = 1.64E-4 $s^{-1}(kGy/h)^{-1}$; EAKT = 0

Confirmation of the model

The empirical model is based on results obtained in dry air at ambient temperature /TAN 70/. This model was recently confirmed by a very similar rate constant of 1.5E-4 $s^{-1}(kGy/h)^{-1}$ at ambient temperature /DIC 03/. It was also shown in /DIC 03/ that the model is also valid in more containment-representative conditions, i.e. a tempera-

ture between 20°C and 80°C, at low and high humidity and even in water, dose rates of 5.5E-3 to 0.56 kGy/h, and initial CH_3I concentrations of 1E-8 to 1E-5 mol/l.

The formation of IO_x (iodate aerosol) from organic iodide decomposition is implicitly considered by the combination of reaction 65 and the I_2/O_3 model.

CH_3 is modelled in gaseous and aqueous phases. The mass transfer of CH_3 from the sump into the atmosphere is calculated by AIM. It is recommended to set the initial value of $CH_3(g)$ to zero in reactor applications.

3.3.3 Iodine reactions with painted surfaces exposed to the gas phase

Inorganic iodine behaviour on dry surfaces

Model

In the containment, dry painted surfaces are an efficient sink for gaseous I_2 due to deposition. From numerous laboratory tests /SIM 97/ and from recent large-scale-tests in the 60 m^3 THAI test facility /LAN 08a/, the reaction of gaseous iodine with painted surfaces can be described as the sequence of two processes: an initial, fast and reversible physisorption process, followed by a chemical reaction of the physisorbed I_2 with the paint producing chemisorbed iodide.

The following formalism was derived from a consistent analysis of the THAI tests Iod-15, Iod-17 and Iod-20 /LAN 08a/:

$$\mathbf{I_2\ (g)} \underset{k(62)}{\overset{k(4)}{\rightleftarrows}} \mathbf{I_2\ (dep,p,g)} \qquad \text{(physisorption)}$$

$$\mathbf{I_2\ (dep,p,g)} \underset{k(77)}{\overset{k(76)}{\rightleftarrows}} \mathbf{I_{chs}\ (dep,p,g)} \qquad \text{(chemisorption)}$$

I_2 (g) molecular iodine in gaseous phase (mol/l)
I_2 (dep,p,g) physisorbed I_2 at painted surface (mol/m^2)
I_{chs} (dep,p,g) chemisorbed iodine at painted surface (mol/m^2)

The corresponding reaction rates are:

$$\frac{d\,I2G}{dt} = -k(4)\cdot I2G\cdot S_{PAINT,G}/V_G + k(62)\,DEPGP\cdot S/(V\cdot 1000)$$

$$\frac{d\,DEPGP}{dt} = -k(4)\cdot I2G\cdot 1000 - k(62)\,DEPGP - k(76)\cdot DEPGP + k(77)\cdot DEPG\_ICHS\cdot 0.5$$

$$\frac{d\,DEPG\_ICHS}{dt} = +k(76)\,DEPGP\cdot 2 - k(77)\,DEPG\_ICHS$$

BAS(4) 4.0E-3 m/s, EAKT(4) = 0

BAS(62) 5.0E-9 s^{-1}, EAKT(62) = 8.22E+4 J/mol

BAS(76) 1.0E-5 s^{-1}, EAKT(76) = 0

BAS(77) rate constant of AIM reaction 77 (s^{-1});
currently set to zero, no value is derived from THAI tests

$S_{PAINT,G}$ painted surface area (m^2)

V_G volume of gaseous phase (m^3)

The model covers the following THAI test conditions:

- Epoxy paint from Geholit & Wiemer,
  (GEHOPON-EXW-E10 with colour RAL 1013)
- coating of a stainless steel plate: 1 primer layer and 2 or 3 paint layers, providing a total thickness of the coating on the steel plate of about 250 µm
- artificially aged at 150 - 160°C for about 24 hours; calculated age of about 15 years
- surface temperature: 80°C to 140°C
- relative humidity at surface temperature: 20 % - 75 %

The Epoxy paint product used in the THAI tests is a follow-up product of the paint used in many German NPP containments.

The given rate constants for resuspension k(62) and chemisorption k(76) are to be considered as rough estimates. Refinements based on the cited THAI tests and irradiated tests (RTF, BIP) are required.

In AIM, the physisorbed I_2 (dep,p,g) and the chemisorbed iodine I_{chs} (dep,p,g) are considered as sources of volatile organic iodide. These reactions are described below.

Inorganic iodine behaviour on wet surface

Wet conditions on surfaces occur with wall condensation. With the condensing steam I_2 is transported towards the wall and deposited onto the paint surface. In general one part of the I_2 stays at the surface and the other part is washed down with the condensate and finally reaches the sump.

The AIM model is based on only two laboratory tests /HEL 96/, performed under the following conditions:

- Epoxy paint GEHOPON E1-1013K
- Ageing of paints: 20 weeks at room temperature or artificial high-temperature ageing to a simulated age of about 10 years
- Condensation rates 4.04E-4 kg/(m^2·s) and 4.36E-4 kg/(m^2·s)
- Temperature 160°C

From these tests, interaction of I_2 with the wet painted surface is modelled by the five processes: 4 (deposition), 62 (resuspension), 44 (wash-down of I_2), 9 (wash-down of I^-), 76 (chemisorption). Figure 3-1 shows these processes schematically.

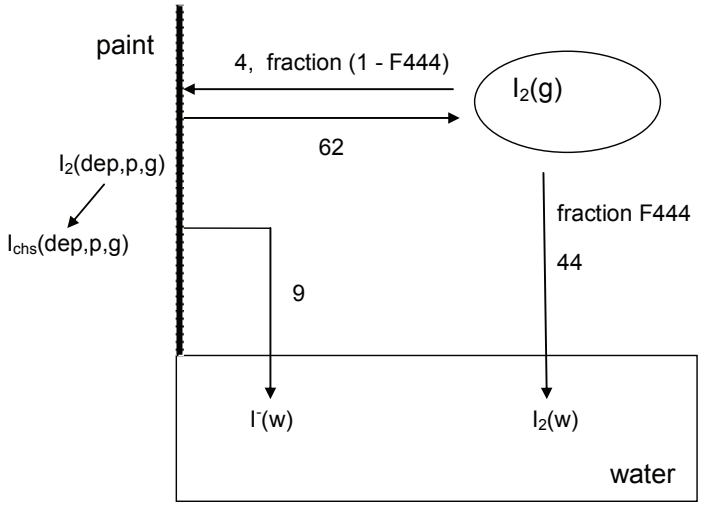

Figure 3-1: Modelling of wet I_2 deposition on paint

Deposition and desorption are formally similar to the dry case

$$\mathbf{I_2\ (g)} \underset{k(62)}{\overset{k'(4)}{\rightleftarrows}} \mathbf{I_2\ (dep,p,g)}$$

Only the part (1.0 – F444) of the totally deposited I_2 is physisorbed onto the paint. The fraction F444 is an input parameter. The other part (F444) of the deposited I_2 is assumed to be immediately transported as I_2 from the painted surface with the draining condensate into the sump. The only short stay of I_2 on the paint is not modelled.

$$\mathbf{I_2\ (g)} \xrightarrow{k(44)} \mathbf{I_2\ (w)}$$

Another part of the I_2 deposited at the painted surface is drained down into the sump as iodide

$$\mathbf{I_2(dep,p,g)} \xrightarrow{k(9)} \mathbf{2\ I^-\ (w)}$$

The associated kinetic equations including conversion of physisorbed into chemisorbed iodine as in dry conditions are

d I2G /dt = - k'(4) · I2G · $S_{PAINT,G}/V_G$
- k(44) · I2G · $S_{PAINT,G}/V_G$
+ k(62) · DEPGP · $S_{PAINT,G}/(V_G \cdot 1000)$

d DEPGP /dt = + k'(4) · I2G · 1000
- k(9) · DEPGP
- k(62) · DEPGP
- k(76) · DEPGP
+ k(77) · DEPG_ICHS · 0.5

d DEPG_ICHS /dt = + k(76) · DEPGP · 2
- k(77) · DEPG_ICHS

d I2 /dt = + k(44) · I2G · $S_{PAINT,G}/V_S$d IMINUS /dt = + k(9) · DEPGP · $(S_{PAINT,G} \cdot 2)/(V_S \cdot 1000)$

BAS(4): 3.1E-3 m/s, EAKT(4) = 0

BAS(9): 2.7E-7 m/s, EAKT(9) = 4.32E+4 kJ/mol

k(62), k(76) and k(77) as in dry conditions, see above

V_G gas volume (m^3)

V_S sump volume (m^3)

k'(4) = k(4) · (1 - F444)

F444 = 0.68

k(44) = k(4) · F444

F444 Fraction of deposited I_2 onto paint which is **immediately** washed down as I_2 into the sump under condensing conditions. The fraction (1-F444) is deposited on the painted surface. Parts of this deposited I_2 can be washed down as I^- afterwards

Model restriction

The selection of "dry condition" or "wet condition" is controlled by the AIM key IRKN (1 = dry, 2 = wet) either by setting IRKN in the input or by calculating it automatically using thermal hydraulic results (see Chapter 5.2.2).

In the model the dependence of the deposition rate k(4) on the condensation rate is not explicitly modelled because the available experimental database includes only cases with strong wall condensation. It is expected that the ongoing analysis of the THAI test Iod-21, performed in April 2008, will provide additional information on the influence of condensation rates, but the evaluation of the test has not been completed yet.

The transition between the models for dry and wet conditions at low wall condensation rates is not as continuous as it should be.

Chemisorbed iodine is not washed down in the current model. This model assumption will be studied in future THAI tests on iodine wash-down from painted surfaces.

Organic iodide release into the gas phase

Volatile organic iodide is released from painted surfaces loaded with iodine. The release is either induced by a thermal process or by radiation. The AIM model is based upon a broad dataset of international laboratory-scale tests, covering the main accident-relevant boundary conditions /DIC 01/ as summarized in Table 3-1.

Table 3-1: Conditions covered by various CH_3I release tests

	Radiation-induced CH_3I release	**Thermal CH_3I release**
Temperature	20 - 80° C	60 - 160° C
Humidity	dry	dry and condensing steam
Loaded species	I_2, I^-	I_2, I^-
Iodine loading	1E-5 – 0.25 mol/m^2	1E-4 – 0.25 mol/m^2
Origin of Epoxy paints	English, French, Finnish	German, English, French
Dose rate	0 - 5 kGy/h	-

The model /FUN 01, DIC 01/ includes the thermal and radiation-induced release of CH_3I from painted surfaces loaded with iodine. The same formalism is applied in AIM for physisorbed iodine I_2 (dep,p,g) and chemisorbed iodine I_{chs} (dep,p,g). The same model is applied for dry and wet painted surfaces. For both, thermal and radiation-induced releases, it is assumed that the rate constant for the I_{chs} reaction is the same as that for the I_2 reaction.

Thermal release of CH_3I

I_2 (dep,p,g) $\xrightarrow{k(14)}$ **2 CH_3I**

I_{chs} (dep,p,g) $\xrightarrow{k(68)}$ **CH_3I**

$$\frac{d\,CH3IG}{dt} = +\,k(14)\cdot(DEPGP\cdot 2)^g \cdot S_{PAINT,G}/(V_G\cdot 1000)$$

$$\frac{d\,DEPGP}{dt} = -\,k(14)\cdot(DEPGP\cdot 2)^g \cdot 1/2$$

$$\frac{d\,CH3IG}{dt} = +\,k(68)\cdot DEPG\_ICHS^g \cdot S_{PAINT,G}/(V_G\cdot 1000)$$

$$\frac{d\,DEPG\_ICHS}{dt} = -\,k(68)\cdot DEPG\_ICHS^g$$

BAS(14) = 1.5E-12 $s^{-1}(m^2/mol)^{g-1}$, EAKT(14) = 7.84E+4 J/mol

k(68) = k(14)

g = 0.5

Radiation-induced release of CH_3I

I_2 (dep,p,g) + γ $\xrightarrow{k(7)}$ **2 CH_3I**

I_{chs} (dep,p,g) + γ $\xrightarrow{k(66)}$ **CH_3I**

$$d\,CH3IG/dt = +k(7)\cdot(DEPGP\cdot 2)^{h}\cdot D_G\cdot S_{PAINT,G}/(V_G\cdot 1000)$$

$$d\,DEPGP/dt = -k(7)\cdot(DEPGP\cdot 2)^{h}\cdot 1/2$$

$$d\,CH3IG/dt = +k(66)\cdot DEPG\_ICHS^{h}\cdot D_G\cdot S_{PAINT,G}/(V_G\cdot 1000)$$

$$d\,DEPG\_ICHS/dt = -k(66)\cdot DEPG\_ICHS^{h}$$

D_G dose rate in the gas phase (kGy/h)

BAS(7) = 3.6E-9 $s^{-1}(kGy/h)^{-1}(m^2/mol)^{h-1}$, EAKT(7) = 1.97E+4 J/mol

k(66) = k(7)

h = 0.426

Due to the large scattering in the underlying database, the uncertainty of the release rate of volatile organic iodide described in /FUN 99/ is determined to be a factor of 10. The values of the rate constants BAS(7) and BAS(14) are those quoted in /FUN 99/ but were multiplied by 7.0. The increase of the constants is due to the experience made in the International Standard Problem ISP-41 /BAL 04/. The constants still lie within the relative broad two-side error band.

3.3.4 Iodine reactions with steel surfaces exposed to the gas phase

Deposition of I_2 onto steel surfaces and the subsequent chemical reaction with steel is an important removal process for volatile iodine from the gas phase e.g. in iodine tests. At wet conditions, i.e. at wall condensation when a draining water film covers the steel surface, a part of the iodine is washed down and transported into the sump.

Dry stainless steel surfaces

From numerous laboratory tests /SIM 97/ and from recent large-scale tests in the 60 m^3 THAI test facility /LAN 08a/, the reaction of gaseous iodine (I_2) with dry stainless steel surfaces can be described as the sequence of two processes: an initial, fast and reversible physisorption process, followed by a slower chemical reaction of the physisorbed I_2 with the steel producing chemisorbed, non-volatile metal iodides (represented by FeI_2).

The following model was derived from a consistent analysis of the THAI tests Iod-6, Iod-7, Iod-9, Iod-16 and Iod-18 /LAN 08a/:

$$\mathbf{I_2\ (g)} \underset{k(63)}{\overset{k(51)}{\rightleftarrows}} \mathbf{I_2\ (dep,s,g)} \text{ (physisorption)}$$

$$\mathbf{I_2\ (dep,s,g)} \underset{k(75)}{\overset{k(74)}{\rightleftarrows}} \mathbf{I_{FeI2}\ (dep,s,g)} \quad \text{(chemisorption)}$$

I_2 (g) molecular iodine in gaseous phase (mol/l)

I_2 (dep,s,g) physisorbed I_2 at stainless steel surface (mol/m^2)

I_{FeI2} (dep,s,g) chemisorbed iodine at stainless steel surface (mol/m^2)

The corresponding reaction rates are:

$$\text{d I2G /dt} = -k(51) \cdot I2G \cdot S_{STEEL,G}/V_G + k(63) \cdot DEPGS \cdot S_{STEEL,G}/(V_G \cdot 1000)$$

$$\text{d DEPGS /dt} = +k(51) \cdot I2G \cdot 1000 - k(63) \cdot DEPGS - k(74) \cdot DEPGS \cdot FSAT + k(75) \cdot DEPG\_FEI2$$

$$\text{d DEPG\_FEI2 /dt} = +k(74) \cdot DEPGP \cdot FSAT - k(75) \cdot DEPG\_FEI2$$

BAS(51) = 2.6E-3 m/s, EAKT(51) = 0

BAS(63) = 1.5E-4 s^{-1}, EAKT(63) = 5.4E+4 J/mol

BAS(74) = 1.0E-4 s^{-1}, EAKT(74) = 0

k(75) rate constant (s^{-1}); AIM reaction 75 is currently switched off by setting BAS(75) to zero; no value is available from THAI tests.

FSAT dimensionless function to describe the influence of humidity on the reaction I_2 (dep,s,g) --> FeI_2 (dep,s,g)

The FSAT function is calculated differently in two ranges of relative humidity (rh in %) and is normalized to 1.0 at rh = 100%.

0 < rh < 40 % rh: FSAT = [5E-7·exp(2.3E-4 (rh + 80)^2)+5E-6] · 2.008E+4

40 < rh < 100 % rh: FSAT = [5.179E-7 · (rh – 40) + 1.872E-5] · 2.008E+4

The model covers the following THAI test conditions:

- stainless steel 1.4571 (AISI/SAE 316 Ti)
- surface temperature: 60°C to 110°C
- relative humidity at surface temperature: 9 % - 80 %. Since the surface wall temperature is in general somewhat lower than the gas temperature, the rh at the surface is somewhat higher than the atmospheric rh.

There is evidence from RTF tests /WRE 99, WRE 00/ that, in the presence of oxygen, I_{FeI2} (dep,s,g) reacts back (reaction no. 75) to I_2 (dep,s,g). At the moment this back reaction is implicitly considered in the forward reaction no. 74. Data for model improvement and validation are expected from the I_2/steel adsorption/desorption tests of the current OECD- BIP project.

Because the painted surface area is much higher than the steel surface area in the reactor containment, the I_2/steel reaction is of minor importance in most reactor calculations. However, the reflective metal insulation (RMI) used in several countries may provide a significant sink for I_2 in reactor containments. Nevertheless, a sophisticated I_2 /steel model is required for interpretation of iodine tests carried out in stainless steel vessels such as RTF, PHEBUS and THAI.

Wet stainless steel surfaces

At wet conditions, i.e. with wall condensation, I_2 is transported towards the wall and deposited onto the steel surface together with the condensing steam, or it is entrained into a falling wall film covering the steel surface. This iodine is washed down into the sump where it is assumed to arrive in iodide form, reflecting a preceding reaction of the I_2 with the steel into water-soluble FeI_2, dissociating into Fe^{2+} and I^-. Hydrolysis of I_2 within the wall film would also partly produce iodide.

Two model options for this effect are available in AIM. In the first option a constant condensation rate is assumed. In the second option the deposition rate is calculated from the variable wall condensation rate determined in the thermal hydraulic part.

Model option 1

Option 1 is used together with IRKN = 2 (permanently wet conditions).

$$\xrightarrow{\text{k(52)}}$$

I_2(g) → [I_2(dep,s,g)] → I^-(w)

In k(52) the processes wet deposition, hydrolysis, and wash-down are modelled together in one single step. It is assumed that all deposited iodine is transported totally and directly into the pool of the zone in which the wall is located. In this option the I_2 deposition is independent from the wall condensation rate.

With IRKN = 2 the default value respectively the input value for k(52) is used.

BAS(52) = 1.35E-3 m/s, EAKT(52) = 0 J/mol

Model option 2

Option 2 is used together with IRKN = 0 (dry or wet conditions). The rate of wet I_2 deposition is calculated by use of the wall condensation rate /WEB 05/. Default and input values for BAS(52) are ignored.

$$k(52) = \frac{R}{1 - e^{-R}}\ k(51)$$

k(52) = k (51) if R = 0 (no wall condensation)

with

$$R = \frac{v_{STEF}}{k(51)}$$

and

$$v_{STEF} = \frac{\dot{m}_{WL,ST}}{\overline{\rho_{ST}} \cdot S_G}$$

v_{STEF} Stefan velocity of condensing steam [m/s]

k(51) I_2 deposition velocity at dry conditions [m/s]

$\dot{m}_{WL,ST}$ wall condensation rate (kg/s)

$\overline{\rho}_{ST}$ average steam density in the boundary layer [kg/m³]

S_G wall surface area in gaseous phase [m²]

BAS(51) = 2.6E-3 m/s, EAKT(51) = 0 J/mol

The Stefan velocity v_{STEF} is calculated internally from thermal hydraulic parameters. At very small wall condensation rates, k(52) becomes k(51) which describes the dry deposition. The model is valid for steel surfaces only and was validated by THAI experiments /WEB 05/.

Model restriction and recommendation

Due to simplifications in the model the wet deposited iodine is transferred from the atmosphere directly into the pool of the zone and not to the walls first. Thus transport of wet deposited iodine by drainage flows into pools outside the zone (e.g. to an external tank) is not possible. The consequence of this restriction can be seen in a calculation on THAI Iod-9 /WEB 09/. An improvement by simulating the I_2 and I^- deposits dissolved in the water film is planned.

It is recommended to use option 2 for wet conditions. Compared to option 1 the dependency of the I_2 deposition rate from the wall condensation rate is considered. In the course of an accident the wall condensation rate varies strongly and becomes locally and/or temporarily zero. With a wall condensation rate of zero, dry conditions are calculated automatically. It is planned to extend the model to other kinds of surfaces.

Wash-down of previous iodine deposits

Iodine deposited onto steel surfaces during dry conditions will be washed down when wall condensation (wet conditions) occurs. This wash-down takes place additionally to the wash-down of freshly deposited iodine. It is modelled in analogy to the wash-down from a painted surface (see reaction no. 9).

Physisorbed I_2 is washed down and arrives in the sump as iodide:

$$\text{d DEPGS /dt} = - k(84) \cdot \text{DEPGS}$$
$$\text{d IMINUS /dt} = + k(84) \cdot \text{DEPGS} \cdot 2 \cdot S/(V_S \cdot 1000)$$

Chemisorbed iodine is washed down and arrives in the sump as iodide:

$$\text{d DEPG\_FEI2 /dt} = - k(85) \cdot \text{DEPG\_FEI2}$$
$$\text{d IMINUS /dt} = + k(85) \cdot \text{DEPG\_FEI2} \cdot 2 \cdot S/(V_S \cdot 1000)$$

For both processes the same rate constant is used which is derived from COCOSYS/AIM-3 calculations on the THAI test Iod-9 /WEB 09/. The rate does not depend on temperature. The iodine wash-off from steel is significantly faster than from paint (k(9)):

$k(84) = 1 \cdot 10^{-4}$ m/s

$k(85) = 1 \cdot 10^{-4}$ m/s

The transformation of previously physisorbed iodine into chemisorbed iodine proceeds as in dry conditions:

$$\mathbf{I_2\ (dep,s,g)} \underset{k(75)}{\overset{k(74)}{\rightleftarrows}} \mathbf{I_{FeI2}\ (dep,s,g)}$$

Wash-down will limit the importance of reactions 74 and 75 and the associated uncertainty of this modelling assumption.

Planned THAI experiments on the wash-down are expected to provide suitable data to improve and/or validate the wash-down model.

3.3.5 Iodine reactions with bare concrete surfaces exposed to the gas phase

Gaseous iodine will deposit onto bare concrete surfaces exposed to a gas phase. With wall condensation including drainage (wet conditions) deposited iodine will additionally be washed down into a sump.

Dry concrete surface

In dry conditions (IRKN = 1) the I_2 (g) deposition on and the resuspension from a concrete surface is modelled in AIM-3 by:

$$\mathbf{I_2\ (g)} \underset{k(64)}{\overset{k(53)}{\rightleftarrows}} \mathbf{I_2\ (dep,c,g)}$$

$$\text{d I2G /dt} = - k(53) \cdot \text{I2G} \cdot S_{CONCR}/V_G + k(64) \cdot \text{DEPGC} \cdot S_{CONCR}/(V_G \cdot 1000)$$

$$d\,DEPGC/dt = +\,k(53) \cdot I2G \cdot 1000 - k(64) \cdot DEPGC$$

Wet concrete surface

In wet conditions (IRKN = 2) the following reaction proceeds to the above mentioned dry surface reactions additionally:

$$\mathbf{I_2\ (dep,c,g)} \xrightarrow{k(54)} \mathbf{2\ I^-\ (w)}$$

Accordingly, the following equations are added to the dry model:

$$d\,DEPGC/dt = -\,k(54) \cdot DEPGC$$

$$d\,IMINUS/dt = +\,k(54) \cdot DEPGC \cdot S_G/(V_S \cdot 1000) \cdot 2$$

The rate constants k(53), k(54) and k(64), as given in Table 4-1, are assumed values and not validated. As bare concrete surfaces are of less interest in most plant applications, no plans exist to remove the uncertainty of this model.

3.4 Interfacial mass transfer and aerosol processes

3.4.1 Mass transfer between gas and water phases at non-boiling conditions

Model

Volatile species are exchanged between gas and water phases by transport processes through the interfacial surface area. These processes are generally abbreviated as "mass transfer".

In AIM-3, the volatile species I_2, CH_3I and CH_3 are considered to participate in the mass transfer process. The mass transfer model is based upon the "two film" theory of diffusion of a volatile species through the interfacial area between two thin boundary layers, one on the gas side and the other on the water side. In stationary conditions, equilibrium between the gaseous and aqueous concentration for each volatile species will be reached. The equilibrium for each species is described by its partition coefficient P,

defined by the ratio of the steady state concentrations in the aqueous and the gaseous phases ($P = c_{w,EQ} / c_{g,EQ}$). P is modelled as function of temperature.

I_2 mass transfer

The rate of change of the I_2(g) concentration due to mass transfer from the sump to the atmosphere at non-boiling conditions is given by:

$$\frac{dI2G}{dt} = k(35) \cdot \frac{S_{W/G}}{V_G} \cdot (I2 - I2G \cdot P(I_2))$$

with

$S_{W/G}$	interfacial surface area water/gas (m^2)
V_G	gas (atmosphere) volume (m^3)

According to /FUR 85/ the temperature dependence of the partition coefficient for I_2 is

$$P(I_2) = 10^{(9.132 \cdot 10^5 \cdot T_W^{-2} - 4.1 \cdot 10^3 \cdot T_W^{-1} + 5.404)}$$

T_W	water (sump) temperature [K]
$P(I_2)$	partition coefficient of I_2 (dimensionless)

The rate constant k(35) is calculated by a two film model using the water side mass transfer coefficient k_W (input parameter: KMTWAS) and the gas side mass transfer coefficient k_G (KMTGAS).

$$\frac{1}{k(35)} = \frac{1}{k_W} + \frac{P(I_2)}{k_G}$$

The recommended values are /EVA 97/:

$K_G = 1.4 \cdot 10^{-3}$ m/s

and

$k_W = 1.0 \cdot 10^{-5}$ m/s

CH_3I mass transfer

The mass transfer of CH_3I between sump and gas phase is calculated in a similar way to I_2, but the partition coefficient is smaller, because CH_3I is much more volatile than I_2:

$$\frac{1}{k(36)} = \frac{1}{k_W} + \frac{P(CH_3I)}{k_G}$$

The partition coefficient for methyl iodide is /BOR 85/

$$P(CH_3I) = e^{-6.97+\frac{2641}{T_W}}$$

T_W water (sump) temperature [K]

For the mass transfer of organic residues (CH_3) the same formalism and values as for CH_3I are used.

Mass transfer correlation

The mass transfer model for non-boiling conditions with two constant coefficients is simple and requires improvements. The model yields a dominating influence of the water-side mass transfer on the exchange between gas and water. However, the water-side mass transfer model does not consider different mixing conditions in the sump which may change the mass transfer coefficient KMTWAS by orders of magnitude. A better mixing of the sump increases the I_2 mass transfer. More specific models correlating the mass transfer coefficient with the mixing conditions have been discussed within the EU-SARNET project /WEB 09/. However, these correlations need further validation with data typical for severe accident conditions. Experimental work on mass transfer is planned within the THAI project on a technical as well as a laboratory scale.

HOI volatility

The volatility of HOI from I_2 hydrolysis in water was discussed controversially, due to contradictory experimental results and conclusions. As in IMPAIR /GÜN 92/, no mass transfer of HOI is considered in AIM-3. Any iodine mass transfer of volatile HOI into the gas phase is implicitly covered by the much more volatile I_2.

3.4.2 Mass transfer between gas and water phases at boiling conditions

Model

In boiling conditions, bubbles will strongly increase the interfacial surface area between gas and water. Therefore, the mass transfer of volatile species from the boiling sump to the gas phase is accelerated efficiently. It is assumed that there is no I_2 mass transfer from the gaseous phase into the sump at boiling conditions.

The rate of change of the I_2(g) concentration at a boiling sump depends on the evaporation rate /STE 91/.

$$\frac{dI2G}{dt} = \frac{VERDAMPF}{\rho_G \cdot V_G \cdot P(I_2)} \cdot (I2 - I2G \cdot P(I_2)) \qquad \text{only for} \quad I2 > I2G \cdot P(I_2)$$

$$\frac{dI2}{dt} = -\frac{dI2G \cdot V_G}{dt \cdot V_W}$$

VERDAMPF	boiling rate in kg/s
ρ_G	density of the gas phase in kg/m^3

Both quantities VERDAMPF and ρ_G are provided from the thermal-hydraulic part in COCOSYS.

In the model the transition from the non-boiling to the boiling condition takes place when the mass transfer rate for boiling exceeds the one for non-boiling. The mass transfer rates for CH3I and CH3 are calculated analogously.

Validation

The mass transfer model for boiling conditions in AIM-3 has not been validated yet. At boiling the aqueous oxygen concentration is assumed to be negligible low. Since O_2(w) is a prerequisite for reactions no. 16 (I^- oxidation by dissolved O_2) and no. 73 (formation of AgO_x by Ag oxidation), these reactions are skipped in the case of sump boiling.

3.4.3 Iodine aerosol deposition and resuspension

For the aerosol species CsI(g), IO_3^-(g), AgI(g) and the silver aerosol Ag(g) deposition and resuspension processes are modelled. The Ag concentration in the sump is needed for calculation of the iodine/silver reaction. The treatment of the aerosol deposition is different in zones without and with a water pool (sump).

Zone without a water pool

In zones **without** a water pool the aerosol species are deposited onto the surfaces. It is not distinguished between floor and walls

$$\textbf{IMINUSG} \underset{k(8)}{\overset{k(5)}{\rightleftarrows}} \textbf{CSI\_AERDEP}$$

k(5) aerosol deposition rate in s^{-1}

k(8) aerosol resuspension rate in s^{-1}, (set to zero)

The deposition process is modelled in the same way for IO3MING, AGIG and AG_G. Three different model options are available in AIM-3 to calculate the aerosol deposition rate k(5) (see below).

A dry resuspension of deposited aerosol is not considered in the model and the reaction constant k(8) is set to zero. In order to simulate a dry resuspension, e.g. as a consequence of a hydrogen deflagration, an extra iodine aerosol injection can be defined in the input.

An empty pool can be refilled with water by wall condensation, drainage or water injection. Then all deposited species will dissolve in the newly created pool.

$$\textbf{CSI\_AERDEP} \xrightarrow{dissolution} \textbf{IMINUSG}$$

The dissolution process is modelled in the same way for IO3MING, AGIG and AG_G.

Zone with a water pool (sump)

In iodine-zones **with** a water pool the species are deposited totally into the water pool (sump). This simulates roughly the settling of iodine aerosol and the subsequent wash-down with wall condensate.

$$\textbf{IMINUSG} \underset{k(8)}{\overset{k(5)}{\rightleftarrows}} \textbf{IMINUS}$$

For IO3MING, AGIG and AG_G the deposition process is modelled in the same way.

When a pool gets empty because of water removal (drainage, pump off) or evaporation, the remaining species in the pool are kept “frozen”, i.e., they do not participate in any chemical reaction or physical process till the pool is filled with water again.

Options to calculate aerosol behaviour

The aerosol behaviour of iodine species can be calculated in three different ways.

KAEJOD = 0: The deposition rate is calculated by use of the given monodisperse aerosol size AEROSZ (iodine input data). Only sedimentation is treated. The deposition rate is assumed to be the same for all aerosol species.

$k_{I^-}(5) = k_{IO3^-}(5) = k_{AgI}(5) = k_{AG}(5)$ monodisperse calculation

KAEJOD = 1: The deposition rate is calculated from the behaviour of the first aerosol component in AERIKA. Important deposition processes and particle growth by condensation are considered. The deposition rate is assumed to be the same for all aerosol species.

$k_{I^-}(5) = k_{IO3^-}(5) = k_{AgI}(5) = k_{AG}(5)$ calculated in AERIKA

KAEJOD = 2: The behaviour of the aerosol components CsI, IO3-, and Ag is calculated individually by the aerosol module AERIKA. Particle size distributions and other properties, e.g. solubility, of these three species may be different. In general the calculated deposition rates are different, only those of AgI is assumed to be the same as for CsI.

$k_{I^-}(5)$, $k_{IO3^-}(5)$, $k_{AG}(5)$ calculated in AERIKA; only IO_3^- release calculated in AIM

$k_{AgI}(5) = k_{I^-}(5)$

The IO_3^- aerosol release rate is calculated from the I_2/ozone reaction (reaction no. 1) in AIM. Therefore with option KAEJOD=2 the size of the primary IO_3^- particles (DIO3) and the standard deviation of the lognormal distribution (SIO3) are iodine input parameters. IO_3^- aerosol injection cannot be defined in the aerosol input, but the IO_3^- aerosol behaviour is treated together with the other aerosol components in AERIKA.

A detailed description of the aerosol behaviour modelling used with the three KAEJOD-options and recommendations for application are given in Chapter 5.3.

Wet resuspension

With a boiling or flashing sump the species in droplet form I^-(drop), IO_3^-(drop), and HOI(drop) are re-entrained from the sump surface to the containment atmosphere (wet resuspension).

$$\textbf{IMINUS} \underset{k(10)}{\overset{k(6)}{\rightleftarrows}} \textbf{IMINUSTR}$$

The iodine species concentration in the droplets is the same as in the sump. k(6) is the re-entrainment factor which is defined by

$$k(6) = \frac{G_{DROP}}{G_{DROP} + G_{ST}}$$

BAS1(6): re-entrainment factor, 1.0E-5 (dim. less)

G_{DROP} droplet mass flow rate, kg/s

G_{ST} steam mass flow rate from the boiling sump, kg/s

One part of the droplets falls back into the sump by sedimentation. This fall back is considered by the rate constant k(10). The net change of the droplet concentration in the gas phase due to re-entrainment and fall back is exemplarily for I^-:

$$\frac{d\ \ IMINUSTR}{dt} = k(6) \cdot IMINUS \cdot \frac{G_{ST}}{V_G} - k(10) \cdot IMINUSTR$$

V_G gas phase volume

BAS(10) droplet fall back, 6.9E-5 s^{-1}

Wet droplet resuspension is activated if the evaporation rate becomes higher than the critical entrainment rate ENTRCR given in the input.

The BAS(6) and BAS(10) values are taken from IMPAIR /GÜN 92/ and are considered to be very coarse. On the basis of THAI tests a new, more precise wet resuspension model for the bubbly flow regime was developed and implemented in COCOSYS. In Chapter 5.3.3 the options to model wet resuspension are discussed in more details.

4 Summary of iodine reaction data

In Table 4-1 the chemical reactions and the physical processes modelled in AIM-3 and the default values for the rate constants and the activation energies are summarized. In the following some explanations on this table are given.

Chemical reaction / physical process

This column gives a short description of the chemical reactions in AIM-3 and their stoichiometry. The following abbreviations are used:

(w)	in the water phase
(g)	in the gas phase
(dp)	as droplets in the gas phase
(dep, paint, w)	deposited on immersed painted surface; analogous for concrete and steel surfaces
(dep, paint, g)	deposited on a painted surface exposed to the gas phase; analogous for concrete and steel surfaces

The hydrogen ion (H^+) and hydroxide ion (OH^-) concentrations indicate a dependence of the reaction on the pH of the water phase. "γ" indicates a radiolytic process, i.e. the reaction depends on the dose rate. The influence of thermal hydraulic parameters like temperature and wall condensation rate can be seen from BAS- and EAKT-values, as described below.

Internal reaction no. (reverse)

The reaction numbers are used code internally in AIM-3. The numbers in brackets indicate reverse reactions.

BAS1, BAS2

BAS1: Regular rate constant at 25 ^{0}C. For gas phase reactions it describes the reaction under **dry** conditions, i.e. without wall condensation.

BAS2: Defined for gas phase reactions only. It is the reaction constant at 25 ^{0}C for **wet** conditions, i.e. with wall condensation.

Reaction rate constants indicated by “calculated” are determined within the code considering dependencies on boundary conditions (e.g. reaction no. 12, 13, 19, 37) which differ from the standard parameterization with the Arrhenius model. Their parameters are internally stored and cannot be changed by input.

Dimension of BAS1/2

Some kinetic equations include variable exponents which are empirical model parameters, like N15, N20, and N29. They are not necessarily integer numbers. These model parameters **must not** be changed without adjusting the rate constants BAS1(15), BAS1(20), and BAS1(29).

EAKT1, EAKT2

EAKT1: Activation energy corresponding to BAS1; for gas phase reactions used only for dry conditions, i.e. without wall condensation [J/mol].

EAKT2: Activation energy corresponding to BAS2; for gas phase reactions used only for wet conditions, i.e. with wall condensation [J/mol]. Not used in sump reactions.

Table 4-1: Chemical and physical rate constants in the iodine model AIM-3

No.	Chemical reactions and physical processes		Internal reaction no. (reverse)	Rate constants / activation energies					Additional information
				BAS1	BAS2 (wall cond.)	Dimension of BAS1/2	EAKT1 [J/mol]	EAKT2 (wall cond.) [J/mol]	
	Water phase reactions								
	Inorganic iodine hydrolysis reactions								
1	I2 hydrolysis (step 1of 2)	I2 (w) + H2O --> HOI (w) + I- (w) + H+	11 (12)	3.00E+00		1/s	7.10E+04		
2	Reverse of I2 hydrolysis (step 1of2)		12 (11)	calc.		1/(M·M·s)	0		T-dependence calc.
3	I2 hydrolysis (step 2of2; HOI disproportionation ("Toth model")	3 HOI (w) --> IO3- (w) + 2 I- (w) + 3 H+	13 (15)	calc.		1/(M·s)	0		
4	Reverse of I2 hydrolysis (step 2of 2; "Dushman reaction"; Toth model)		15 (13)	1.10E+05		1/(M·M·M**N15·s)	3.10E+04		N15 = 1.0
5	I- oxidation by dissolved O2	2 I- (w) + 1/2 O2 (w) + 2 H+ --> I2 (w) + H2O	16	1.00E-07		1/(M·s)	4.60E+04		O2(w) not modelled
	Inorganic iodine radiolysis reactions								
6	Radiolytic I2 formation from I-	2 I-(w) + γ --> I2(w)	20 (21)	2.20E-05		1/(M**N20·kGy/h·s)	0		N20 = 0.2
7	Reverse of radiolytic I2 formation from I-		21 (20)	1.00E-04		1/s	0		
8	Radiolytic I2 formation from IO3-	IO3- (w) + γ --> I2 (w)	29 (34)	2.20E-05		1/(M**N29·kGy/h·s)	0		N29 = 0.2
9	Reverse of radiolytic I2 formation with IO3-		34 (29)	1.00E-04		1/s	0		
	Silver / iodine reactions								
10	AgI formation from Ag + I2	I2 (w) + 2 Ag (w) --> 2 AgI (w)	28	2.00E-01		m /(M·s)	0		RR calc. f(Ag, Par.S)
11	AgI formation from AgOx + I-	AgOx (w) + I- (w) --> AgI (w)	56	2.00E+00		m /(M·s)	0		RR calc. f(AgOx, Par.S)
12	Formation of AgOx by Ag oxidation	Ag(w) + O2 --> AgOx(w)	73	8.70E-09		mol/(m2·s)	0		
13	Radiolytic AgI destruction	AgI (w) + γ --> I2 (w) + Ag (w)	26 (27)	0		1/(kGy/h·s)			currently not considered
14	Reverse of radiolytic AgI destruction		27 (26)	0		1/s			currently not considered
	Homogeneous organic iodine reactions in the water phase								
15	Thermal CH3I formation from I2	I2 (w) + 2 CH3 (w) --> 2 CH3I (w)	22 (23)	1.5 E+00		1/(M·s)	2.10E+04		
16	Reverse of thermal CH3I formation from I2		23 (22)	0		1/s			

No.	Chemical reactions and physical processes		Internal reaction no. (reverse)	Rate constants / activation energies					Additional information
				BAS1	BAS2 (wall cond.)	Dimension of BAS1/2	EAKT1 [J/mol]	EAKT2 (wall cond.) [J/mol]	
17	Thermal CH3I formation from HOI	HOI (w) + CH3 (w) --> CH3I (w)	40 (41)	1.0 E-01		1/(M·s)	2.00E+04		
18	Reverse of thermal CH3I formation from I2		41 (40)	0		1/s			
19	Radiolytic CH3I destruction	2 CH3I (w) + γ --> I2 (w) + 2 CH3 (w)	24 (25)	3.00E-04		1/(kGy/h·s)	0		
20	Reverse of radiolytic CH3I destruction		25 (24)	0		1/(M·s)			
21	Hydrolysis of CH3I by H2O	CH3I (w) + H2O --> I- (w) + CH3OH + H+	30 (31)	1.50E-07		1/s	1.20E+05		
22	Reverse of hydrolysis of CH3I by H2O		31 (30)	0		1/(M·M·s)			
23	Hydrolysis of CH3I by OH-	CH3I (w) + OH- --> I- (w) + CH3OH	32 (33)	5.70E-05		1/s	9.20E+04		
24	Reverse of hydrolysis of CH3I by OH-		33 (32)	0		1/(M·s)			
	Iodine reactions with immersed painted surfaces								
25	I2 deposition on paint	I2(w) --> I2(DEP,paint,w)	17	2.00E-06		m/s	9.59E+03		
26	I2 dissolution from paint after I2 deposition	I2 (DEP,paint,w) --> I2 (w)	38	T ≤ 90 °C: 4.16E-09		1/s	8.55E+04	0	T > 90 °C: K(38) = 2,0E-6
27	I- dissolution from paint after I2 deposition	I2(DEP,paint,w) --> I-(w)	69	8.58E-07		1/s	5.10E+04		
28	I- deposition on paint	I- (w) --> I- (DEP,paint,w)	37	calc.	calc.	m/s	calc.		pH-, AGE-dependent
29	I- dissolution from paint after I- deposition	I- (DEP,paint,w) --> I- (w)	19	calc.	calc.	1/s	calc.	0	pH-, AGE-dependent
30	Chemisorbed I- from physisorbed I-	I- (DEP,paint,w) --> ICHS (DEP,p,w)	79 (80)	calc.		1/s	0		pH- and T-dependent
31	Thermal CH3I dissolution from paint	I2 (DEP,paint,w) --> CH3I (w); I- (DEP,paint,w) --> CH3I (w) ICHS (DEP,paint,w) --> CH3I (w)	39	1.50E-12		$1/s \cdot (m^2/mol)^{g-1}$	7.84E+04		g = empirical exponent
32	Radiolytic CH3I dissolution from paint	I2 (DEP,paint,w) + γ --> CH3I (w); I- (DEP,paint,w) + γ --> CH3I (w) ICHS (DEP,paint,w) + γ --> CH3I (w)	18	3.60E-09		$1/(kGy/h \cdot s) \cdot (m^2/mol)^{h-1}$	1.97E+04		h = empirical exponent
	Iodine reactions with immersed steel surfaces								
33	I2 conversion to I- at steel surface	I2 (w) + steel (w) --> I- (w)	55	1.25E-07		m/s	8.08E+04		
	Iodine reactions with immersed concrete surfaces (non-painted)								
34	I2 deposition on concrete	I2 (w) --> I2 (DEP,concrete,w)	57	2.00E-05		m/s	0		
35	I- dissolution from concrete	I2 (DEP,concrete,w) --> I- (w)	58	1.00E-02		1/s	0		

No.	Chemical reactions and physical processes		Internal reaction no. (reverse)	Rate constants / activation energies					Additional information
				BAS1	BAS2 (wall cond.)	Dimension of BAS1/2	EAKT1 [J/mol]	EAKT2 (wall cond.) [J/mol]	
	Gas phase reactions								
	Iodine/ozone reaction								
36	Formation of IO3-(g) by reaction of I2 and O3	I2 (g) + O3 --> IO3- (g)	1	2.40E+03		1/(M·s)	2.50E+04		
37	Radiolytic destruction of IO3-(g)	2 IO3- (g) + γ --> I2 (g)	2	2.30E-06		1/(kGy/h·s)	0		
38	Radiolytic O3 formation	atmosphere + γ --> O3 (g)	71 (72)	4.70E-11		M/(kGy/h·s)	0		
39	Radiolytic O3 decay	O3 (g) + γ --> O2	72 (71)	4.30E-02		1/(kGy/h·s)	1.12E+04		
40	O3 decomposition on painted surfaces	O3 (g) --> -	82	1.27E-05		m/s	5.83E+04		
41	O3 decomposition on steel surfaces	O3 (g) --> -	83	1.46E-05		m/s	5.62E+04		
42	Thermal O3 decay	O3 (g) --> O2	78	3.0E-04		1/s	5.81E+04		
	Homogeneous organic iodine reactions in the gas phase								
43	Radiolytic CH3I decomposition	CH3I (g) + γ --> ½ I2 (g) + CH3 (g)	65 (67)	1.64E-04		1/(kGy/h·s)	0		
44	Reverse of radiolytic CH3I decomposition	I2 (g) + 2 CH3 (g) --> 2 CH3I (g)	67 (65)	0		1/(M·s)	0		
	Iodine reactions with painted surfaces exposed to the gas phase								
45	I2 deposition on dry and wet paint	I2 (g) --> I2 (DEP,paint,g)	4 (62)	4.0E-03	3,10E-03	m/s	0	0	Par. F444=0.68
46	I2 resuspension from dry and wet paint	I2 (DEP,paint,g) --> I2 (g)	62 (4)	5.0E-09	8.8E-08	1/s	8.22E+04	2.72E+04	
47	Physisorbed I2 into chemisorbed iodine	I2 (DEP,paint,g) --> ICHS (DEP,p,g)	76 (77)	1.0E-5	1.0E-5	1/s	0	0	
48	reverse of reaction 76	ICHS (DEP,p,g) --> I2 (DEP,paint,g)	77 (76)	0		1/s	0		
49	I2 transport to wet paint and subsequent wash-down to sump as I2	I2 (g) --> I2 (DEP,paint,g) --> I2 (w)	44	0	3,10E-03	m/s	0	0	Par. F444=0.68
50	Wash-down from paint to sump as I- in condensing conditions	I2 (DEP,paint,g) --> I- (w)	9	0	2,70E-07	1/s	0	4.32E+04	
51	Thermal CH3I release from physisorbed iodine	I2 (DEP,paint,g) --> CH3I (g)	14	1.50E-12		$1/s\cdot(m^2/mol)^{g-1}$	7.84E+04		g = empirical exponent
52	Radiolytic CH3I release from physisorbed iodine	I2 (DEP,paint,g) + γ --> CH3I (g)	7	3.60E-09		$1/(kGy/h\cdot s)\cdot(m^2/mol)^{h-1}$	1.97E+04		h = empirical exponent
53	Thermal CH3I release from chemisorbed iodine	ICHS (DEP,paint,g) --> CH3I (g)	68	1.50E-12		$1/s\cdot(m^2/mol)^{g-1}$	7.84E+04		g = empirical exponent
54	Radiolytic CH3I release from chemisorbed iodine	ICHS (DEP,paint,g) + γ --> CH3I (g)	66	3.60E-09		$1/(kGy/h\cdot s)\cdot(m^2/mol)^{h-1}$	1.97E+04		h = empirical exponent

No.	Chemical reactions and physical processes		Internal reaction no. (reverse)	Rate constants / activation energies					Additional information
				BAS1	BAS2 (wall cond.)	Dimension of BAS1/2	EAKT1 [J/mol]	EAKT2 (wall cond.) [J/mol]	
	Iodine reactions with steel surfaces exposed to the gas phase								
55	I2 deposition on dry steel	I2 (g) --> I2 (DEP,steel,g)	51 (63)	2.6E-03	0	m/s	0	0	
56	Resuspension from dry steel	I2 (DEP,steel,g) --> I2 (g)	63 (51)	1.5E-04	0	1/s	5.40E+04	0	
57	I2 deposition on wet steel, FeI2 formation, and wash-down to sump as I-	I2 (g) --> I- (w)	52	calc.	1.35E-03	m/s	0	0	option no. 2 / 1
58	Physisorbed I2 into chemisorbed iodine	I2 (DEP,s,g) --> FEI2 (DEP,s,g)	74 (75)	1.0E-04	0	1/s	0		Par. FSAT calc.
59	Reverse reaction 76	FEI2 (DEP,s,g) --> I2 (DEP,s,g)	75 (74)	0		1/s	0		
60	Wash-down of I2 (DEP,steel,g) to sump as I- in condensing conditions	I2 (DEP,s,g) --> I- (w)	84	0	1.0E-04	1/s	0	0	
61	Wash-down of FEI2 (DEP,steel,g) to sump as I- in condensing conditions	FEI2 (DEP,s,g) --> I- (w)	85	0	1.0E-04	1/s	0	0	
	Iodine reactions with bare concrete surfaces exposed to the gas phase								
62	I2 deposition on dry concrete	I2 (g) --> I2 (DEP,concrete,g)	53 (64)	2.50E-03	2.50E-03	m/s	0	0	
63	I2 resuspension from dry concrete	I2 (DEP,concrete,g) --> I2 (g)	64 (53)	6.00E-06	6.00E-06	1/s	1.00E+04	1.00E+04	
64	I2 deposition on wet concrete, hydrolysis, and wash-down to sump as I-	I2 (DEP,concrete,g) --> I- (w)	54	6.00E-03	6.00E-03	1/s	0	0	
	Interfacial mass transfer and aerosol processes								
	Mass transfer between gas and water phases								
65	I2 transfer through the interface sump - gas	I2 (w) <==> I2 (g)	35	calc.		m/s	0		
66	CH3I and CH3 transfer through the interface sump - gas	CH3I (w) <==> CH3I (g); CH3 (w) <==> CH3 (g)	36	calc.		m/s	0		
	Iodine aerosol deposition and resuspension								
67	Deposition of gasborne aerosols I-, AgI and IO3- on floor	I-(g), AgI(g) and IO3-(g) --> I-(DEP,g), AgI (DEP,g) and IO3-(DEP,g)	5 (8)	6.90E-05		1/s	0		option KAEJOD=0
68	Resuspension of aerosols I-, AgI and IO3- to gas phase	I-(DEP,g), AgI (DEP,g) and IO3-(DEP,g) --> I-(g), AgI(g) and IO3-(g)	8 (5)	0		1/s	0		
69	Reentrainment of droplets I-(dp), HOI(dp) and IO3-(dp) from sump	I-(w), AgI (w) and IO3-(w) --> I-(dp,g), AgI (dp,g) and IO3-(dp,g)	6 (10)	1.00E-05		dim.less	0		

No.	Chemical reactions and physical processes		Internal reaction no. (reverse)	Rate constants / activation energies					Additional information
				BAS1	BAS2 (wall cond.)	Dimension of BAS1/2	EAKT1 [J/mol]	EAKT2 (wall cond.) [J/mol]	
70	Fall back of droplet I-(dp), HOI(dp), IO3-(dp) from gas to sump	I-(dp,g), AgI (dp,g) and IO3-(dp,g) --> I-(w), AgI (w) and IO3-(w)	10 (6)	6.90E-05		1/s	0		

Abbreviations

AGE	age of paint	M	mol/l
calc.	calculated internally in the code	Par.	parameter
γ	energy from ionising radiation	RR	reaction rate

5 Coupling within COCOSYS

In COCOSYS all main interaction processes between iodine chemistry, thermal hydraulics and aerosol physics are modelled by tight numerical couplings of the modules on a time step level. The interaction processes considered are:

- Thermal hydraulic boundary conditions for chemical reactions and physical processes treated in AIM
- Aerosol behaviour of particulate iodine species
- Inter-compartmental iodine transport by gas and water flows
- Feedback of iodine decay heat on thermal hydraulics and aerosol physics

The iodine nodalisation can be defined differently for the nodalisation used for the thermal hydraulic and the aerosol problems. Specific iodine requirements, i.e. a lower spatial resolution, and/or a sufficiently large gas space above each sump, can be met. Additionally computational time can be saved.

5.1 Separate iodine nodalisation

In COCOSYS-AIM calculations the user can apply the thermal hydraulic nodalisation as it is for the iodine problem or he can create an own iodine nodalisation with a reduced number of zones. Two or several thermal hydraulic zones are combined to one iodine zone. The rules for this re-nodalisation are listed in Table 5-1. In a COCOSYS-AIM calculation both nodalisations are used simultaneously. In Figure 5-1 a thermal hydraulic/aerosol nodalisation (cloured areas) with a separate iodine nodalisation (red frames) is depicted.

Table 5-1: Rules for a separate iodine nodalisation

Part	Rule
Sump	The sump of an iodine zone can consist of one or several equilibrium sump zones (NZSU > 0) or of the sump part of one non-equilibrium zone. If several equilibrium sump zones are combined, their sump numbers NZSU must be equal (and greater than zero).
Atmospheric zone / junction	– The atmospheric part of an iodine zone consists of equilibrium zones (all with NZSU = 0) and/or the atmospheric part(s) of non-equilibrium zones. – The combined gas parts of zones have to be connected via atmospheric junctions. But these junctions are not used for iodine transport. – Only junctions connecting different iodine zones are used for iodine transport.
Environment	– An environment iodine zone consists of one or several thermal hydraulic environment zones. At least one environment iodine zone has to be defined.

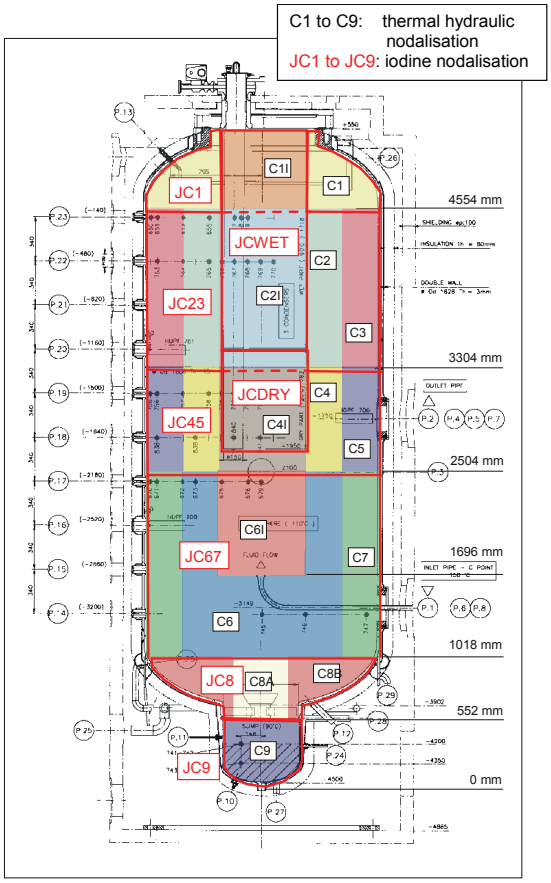

Figure 5-1: Example for a separate iodine nodalisation (PHEBUS-FP containment).

Three different types of iodine zones can be used:

- A+S: iodine-zone with gaseous part and liquid part (sump). Chemistry in the liquid part is only calculated if it contains sufficient water (water level > CRTHE)
- ATM only gaseous part (no sump)
- ENV environment iodine-zone

Only equilibrium zones with NZSU = 0 (no sump zone) can be assigned to ATM type iodine zones.

When several zones are combined to an iodine zone the thermal hydraulic parameters (temperature, relative humidity, wall condensation rate, gas and aerosol concentrations) are averaged.

In AIM the chemical equations are solved explicitly for each iodine zone. AIM is coupled to the thermal hydraulic and aerosol modules in a quasi-stationary way. High intercompartmental mass flows can cause iodine mass balance errors. These errors can be controlled in most cases by a reduction of the iodine time step DZLIM in the input data. In multi-compartment calculations the DZLIM value should not exceed 10 s.

5.2 Interactions with thermal hydraulics

The influence of temperature on the reaction rates is generally described by the Arrhenius equation (Chapter 3.1). Gas and water phase temperatures are delivered by the thermal hydraulic module. Separate wall temperatures are not considered in AIM.

5.2.1 Atmospheric iodine transport

The transport of gaseous and particulate iodine in a COCOSYS multi-compartment configuration is calculated under the following assumptions:

- The flow velocity of the gases and aerosol particles in the connections is the same. The only exception is the slip of particles at slow flows in vertical connections.
- The complete gaseous and particulate iodine is in the zones. The connections are free of any mass.
- In the connections no iodine and aerosol deposition takes place.

The transport of gaseous and particulate iodine is simulated in each zone by sources and sinks corresponding to the inflow and outflow of iodine species from and into neighbouring zones, respectively.

$$V_i \frac{dc_{i,k}}{dt} = \sum_{l=1}^{l\max} V_l \frac{c_{l,k} \cdot G_{l \to i}}{m_{G,l}} - \sum_{m=1}^{m\max} V_m \frac{c_{i,k} \cdot G_{i \to m}}{m_{G,i}}$$

$\frac{dc_{i,k}}{dt}$	time derivative of iodine species k in zone i following the aerosol transport into and from neighbouring zones [mol/l/s]
$c_{l,k}$	iodine species concentration k in zone l [mol/l]
$c_{i,k}$	analogous
$G_{l \to i}$	atmospheric mass flow in the connection between zone l and zone i [kg/s]
$m_{G,l}$	total gas mass in zone l [kg]
V_G	zone volume [m^3]
l_{max}	number of inflows
m_{max}	number of outflows

The individual iodine zones are tightly (explicitly) coupled in COCOSYS-AIM. The time integration of the iodine reactions is carried out in succession in the individual zones.

It has to be noted that the change in the iodine concentration $\frac{dc}{dt}$ due to the transport in a closed containment is generally small. In the case of large mass flows (e.g. with forced convection), the concentration differences between the zones are small, and larger concentration differences are only maintained with slight flows (stratification). The length of the iodine time step is not controlled. It has to be reduced in case of a significant iodine mass balance error.

5.2.2 Dry and wet conditions

In the gas phase with **wall condensation** (wet conditions) different or additional iodine reactions occur as compared to dry conditions (Chapter 3.2). With wet conditions the second set of reaction constants BAS2 is used. The use of BAS2 can be either forced

by setting the key IRKN = 2 or determined automatically in each time step individually for each iodine-zone (IRKN=0). With the latter option wet conditions are achieved if the wall condensation rate exceeds the threshold ACOND given in the input.

$$\frac{\dot{m}_{COND,ST}}{S_G} \leq ACOND \quad \rightarrow \quad \text{dry conditions, BAS1 constants used}$$

$$\frac{\dot{m}_{COND,ST}}{S_G} > ACOND \quad \rightarrow \quad \text{wet conditions, BAS2 constants used}$$

$\dot{m}_{COND,ST}$ wall condensation rate in iodine-zone, kg/s

S_G surface area in gaseous phase iodine-zone, m²

ACOND threshold for specific wall condensation rate [kg/(m²s)]; input parameter; $1 \cdot 10^{-4}$ kg/(m²s) is recommended

For the I_2 deposition on a steel surface by wall condensation the deposition velocity is calculated directly from the wall condensation rate delivered by the thermal hydraulic module (s. Chapter 3.3.4).

5.2.3 Iodine wash-down

Molecular and particulate iodine deposited on surfaces is washed down by draining condensate into the sumps. With wall condensation I_2 (g) is directly transferred to the sump as I_2 from painted surfaces (Chapter 3.3.3) or as I^- from steel and concrete surfaces (Chapter 3.3.4 and 3.3.5). I_2 deposited during a dry period will be washed down with wall condensate in a wet period.

The wash-down of deposited particulate iodine species is possible with all three options available for iodine aerosol treatment (Chapter 5.3). In each iodine zone the aerosols are first washed to the zone pools (residual water) and from there to the sump. A prerequisite is the specification of the drain junctions.

Small pools may dry out when the water is pumped off, drained or evaporated. If the sump water level H falls below the critical sump height CRTHE the calculation of iodine chemistry is stopped.

- The dissolved, suspended and deposited iodine masses including I_2 and CH_3I are kept constant (“frozen”) until iodine chemistry in the sump is reactivated (H > CRTHE).

For a highly concentrated sump the modelled iodine chemistry in AIM is not valid any more. Therefore the critical sump volume (and CRTHE) should not be chosen too small. A reasonable limit seems to be $1 \cdot 10^{-2}$ m.

5.2.4 Removal by spray

If a spray system is activated, the wash-out of iodine aerosols and volatile species (I_2 and CH_3I) is calculated. The model for the wash-out of gaseous species uses the mass transfer coefficient beteeen sump and atmosphere (according to Chapter 3.4.1) and considers the concentration increase in the spray droplets along the falling height ΔH /KLE 09a/.

$$c_{DROP} = I2G \cdot P(I_2) + \left(c_{DROP,0} - I2G \cdot P(I_2)\right)\exp\left(-\frac{3 \cdot k(35)}{v_{DROP} \cdot r_{DROP}} \cdot \Delta H\right)$$

$c_{DROP,0}$, c_{DROP}	I_2 concentration in droplets at beginning and end of path [mol/l]
ΔH	total falling height inside path [m]
v_{DROP}	initial spray droplet velocity [m/s]
r_{DROP}	initial spray droplet radius [m]
k(35)	I_2 mass transfer coefficient atmosphere/sump [m/s]
$P(I_2)$	partition coefficient for I_2

The mean I_2 mass transfer rate is then determined by use of the concentration difference between top and end of the spray path and the droplet volume flow.

$$\frac{dm(I_2)}{dt} = \left(c_{DROP} - c_{DROP,0}\right) \cdot \dot{V} \quad \text{[kmol/s]}$$

The washed out iodine is always transported into the water pool/sump of the lowest zone defined in the spray system. There it can participate in chemical reactions or can be transported further on by drainage or pumps.

$$I2G \xrightarrow{SPRAY} I2 \text{ (lowest zone)}$$

The wash-out of organic iodide CH3IG by a spray system is calculated in the same way. It is less efficient than the I_2 wash-out due to the lower partition coefficent. The wash-out of organic residues CH3G is not considered. Chemical reactions in the spray droplets are not treated.

If spontaneous evaporation of droplets take place I_2 and CH_3I are transferred into the atmosphere corresponding to the evaporated volume fraction of droplets. The release of organic residues is not yet treated.

In case of option KAEJOD = 2 (detailed aerosol calculation with AERIKA) the wash-out of the particulate species CsI and IO_x is calculated by the spray model in the aerosol module.

5.3 Iodine aerosol behaviour

In AIM the four iodine aerosol species CsI (or I^-), IO_3^-, AgI and Ag are treated. Three model options with different simplifications are available (Table 5-2). The options are recommended for different applications.

Table 5-2: Model options for iodine aerosol treatment

Option	Simplifying assumption	Restrictions	Application
KAEJOD = 0 Monodisperse calculation	- Constant mean particle size AEROSZ - Sedimentation only - No condensation on particles	Dry resus-pension and wash out by spray not modelled	For rough estimations

	- Same deposition rate for I^-, IO_3^-, AgI, and Ag		
KAEJOD = 1 Well mixed approach	- All components well mixed - Same deposition rate for I-, IO_3^-, AgI, and Ag	none	Cases with high aerosol concentration (> 1g/m³). Suited for the aerosol phase in many severe accident scenarios
KAEJOD = 2 Multi-component calculation	- CsI, IO_3^- and Ag modelled by AERIKA - Deposition rate for AgI as for CsI	none	Accurate aerosol calculation for CsI, IO_3^- and Ag. For cases with low concentrations. For evaluation of tests.

Monodisperse calculation

In this option only aerosol depletion by sedimentation is regarded:

$$\frac{dc_i}{dt} = -k(5)c_i$$

k(5) effective aerosol deposition coefficient [1/s]

c_i concentration of iodine species i [mol/l]

$$k(5) = \frac{FSED}{V_G} v_{SED}(D_P)$$

D_P mean particle diameter [m]

v_{SED} sedimentation velocity [m/s]

FSED floor area also used as sump surface [m^2]

V volume [m^3]

D_P is given in the input (AEROSZ). The sedimentation velocity v_{SED} is calculated by Stoke's formula with the Knudsen-Weber-correction.

$$v_{SED} = \frac{D_P^2 \rho_P g}{18 \eta \chi}\left(1 + \frac{2\lambda}{D_P}\left(F_{SL} + 0.4e^{-1.1\frac{D_P}{2\lambda}}\right)\right)$$

ρ_P density of aerosol material [kg/m^3]

g gravitational acceleration [m/s^2]

η	dynamic viscosity of atmosphere, [Pa·s]
λ	mean free path of gas molecules [m]
χ	dynamic shape factor
F_{SL}	slip factor (= 1.37)

In the monodisperse model the dynamic shape factor is set to 1.0 (spherical particles) and the density is set to 2500 kg/m^3.

The sedimentation velocity of wet **resuspended droplets** (re-entrainment, reaction no. 10) is also calculated by the Stoke's formula but without the correction term. The droplet size is given by the input parameter DROPSZ. The resulting deposition rate overwrites the default value BAS(10).

The deposition rate of resuspended droplets calculated by the monodisperse model is also used for the options KAEJOD = 1 and KAEJOD = 2.

5.3.1 Well-mixed aerosol approach

In this option a core melt aerosol in a high concentration which agglomerates with the iodine aerosols is assumed. Under these conditions the behaviour of the iodine aerosols is governed by the behaviour of the core melt aerosol. The deposition of all three iodine aerosols is calculated by use of the deposition rate derived from the first aerosol component in the aerosol module AERIKA. Sedimentation, diffusive deposition, thermophoresis, diffusiophoresis as well as condensation on particles are considered.

The total deposition rate α(t) [1/s] in a time step Δt is approximated by

$$\alpha(t) = \frac{\Delta m_{DEP}}{\bar{c} V_G \Delta t}$$

$$= k(5)$$

Δm_{DEP}	deposited aerosol mass in the time step Δt [kg]
V_G	gas volume, [m^3]
$\bar{c}$	average aerosol concentration in the time step [kg/m^3]
Δt	aerosol time step, [s]

If the concentration of the first aerosol component is (temporarily) zero the iodine deposition is calculated as in option KAEJOD = 0.

5.3.2 Aerosol calculation in detail

With option KAEJOD = 2 the most precise calculation of the iodine aerosol behaviour is made. The hygroscopic aerosol CsI and the fine disperse IO_3^-, which is a product of the radiolytic I_2 oxidation, are calculated as separate components by the module AERIKA. All essential aerosol processes like agglomeration, particle growth by condensation, hygroscopic effect, sedimentation, diffusion and diffusiophoresis are taken into account. For the wash-down of the species the wall condensation rates calculated within the thermal hydraulic module are used. This option requires the largest computational effort especially if condensation on the particles is treated.

The Ag aerosol is modelled as a separate component in order to accurately calculate the Ag distribution in the containment and especially its concentration in the sump.

This option KAEJOD = 2 is recommended for reactor scenarios with a low concentration of a background aerosol, e.g. degraded core accidents. This option is also suited for a precise evaluation of certain experiments.

The ordering of the aerosol components with this option is fixed to:

IMINUSG (CsI) = 1st AERIKA component

IO3MING (IO_3^-) = 2nd AERIKA component

AG_G (Ag) = 3rd AERIKA component

On the fourth and higher positions (maximum eight) other aerosol components can be simulated with AERIKA. The behaviour of AgI is calculated in a simplified way by the deposition rate of the first AERIKA aerosol component (CsI).

For I^- and Ag a complete aerosol calculation including the iodine aerosol injection is performed in AERIKA. The injection of the iodine aerosol species in AIM is ignored. The IO_3^- aerosol formation is calculated in AIM from the I_2/ozone reaction, but the IO_3^- behaviour is also treated in AERIKA. Information on the IO_x particle size distribution

(parameters DIO3 and SIO3) has to be given in the iodine input. Different nodalisations for AIM and AERIKA are considered.

In the output of the aerosol mass balance (BALANCE) the IO_x mass is added to position no. 5 (RESUSPEN) and not, as may be expected, to position no. 1 (INJECTION).

The deposited iodine can be washed down with draining condensate into sumps. In iodine zones with a sump the total of the deposited aerosol mass is transferred into the liquid part, where the species can react further.

5.3.3 Resuspension

Dry resuspension

Dry resuspension of deposited aerosol can take place with strong air flows as expected e.g. during a hydrogen deflagration. The resuspension process is simulated by regarding the aerodynamic forces and adhesive forces acting on particles in a multilayer particle bed. The particle size distribution of the resuspended aerosol has to be given in the input. A unimodal or a bimodal particle size distribution can be chosen. Iodine and other aerosols are resuspended with the same fraction, i.e. the components are assumed to be well mixed in the particle bed.

$$CSI\_AEDEP \cdot S_{FL,DRY} \xrightarrow{fresus} IMINUSG \cdot V$$

$S_{FL,DRY}$	floor area in zones without a sump, m²
f_{resus}	resuspenspended fraction

Dry resuspension can only be calculated in zones without a sump. f_{resus} is determined by the model. The resuspension of the species IO3_AEDEP and AG_AEDEP is determined analogously.

The simulation of dry resuspension is only possible with KEYJOD=2. The model is initalized in the input by the keyword “LRESO“ in the aerosol data (“K---AEROSOLS). A description of the model and the input data is given in /KLE 09a/. The model was validated on the tests VANAM-M4 and the THAI tests Aer-1, Aer-3 and Aer-4 /SPE 09/.

Wet resuspension

When gas is flowing through a pool, e.g. with boiling, droplets are formed at the surface and transported with the rising gas flow into the atmosphere. Together with the droplets soluble and insoluble fission products are released in aerosol form to the atmosphere. This process is called re-entrainment or wet resuspension.

Droplet generation depends essentially on the superficial velocity of the gas flow through the pool. At low superficial velocities the gas flow consists of single bubbles rising through the pool (bubbly flow) and bursting at the surface. At high superficial velocities bubbles of different sizes and shapes rise in a turbulent way (churn turbulent flow) producing hollow columns of liquid, whose upper part rapidly disintegrates into droplets.

Three options are available in AIM to model wet resuspension of the particulate iodine species. The input requirements and the accuracy of these models are different.

Option 1: Simple model with constant resuspension rate

This resuspension model is activated when the sump evaporation rate exceeds the input parameter ENTRCR. Then the constant resuspension rate k(6) and the fall back rate are used to calculate the net release of IMINSTR, IO3TR, and HOITR in droplet form in to the gas phase. It is not distinguished between the bubbly and the churn turbulent flow regime. The option is described in more detail in Chapter 3.4.3

If one of the two other options, which are only possible with KAEJOD=2, is chosen, the simple model has to be switched off, e.g. by use of a large ENTRCR value.

Option 2: User defined resuspension factor

In this option user defined resuspension factors can be provided. This option works on the iodine model AIM (option KEYJOD=2) and on the fission product transport model FIPHOST. Based on the iodine resuspension rate a corresponding aerosol release above the sump will be calculated. This iodine release is an additional release, that means the resuspended iodine mass is not removed from the iodine mass in the sump mass.

In the iodine module the resuspended masses are balanced in the separate iodine species I-_DROPS, IO3-_DROPS and HOI. The deposition of these droplets is determined by the droplet size DROPSZ specified in the AIM module data.

More details on this options can be seen in /KLE 09a/.

Option 3: Resuspension correlation from RUB

On the basis of the 4 THAI wet resuspension tests TH-14 to TH-17 a semi-empirical correlation between resuspension rate and superficial velocity was developed at the Ruhr-Universität Bochum (RUB, Institute LEE) /DAP 08/. The droplets are assumed to be released to the atmoshere as dried solid particles with a log normal size distribution and user defined diameter and standard deviation. Depending on the superficial velocity two sets of parameters are defined for two flow regimes. The transition is assumed to be at a superficial velocity of 0.05 m/s. A detailed description of the model and the parameters are given in /KLE 09a/.

Model restriction

The RUB correlation describes the release of submicron film particles in the bubbly flow and beginning churn turbulent flow regime. Not covered is the high particle release in the strong turbulent flow regime.

Under atmospheric conditions above the sump other than in THAI, e.g. with a higher gas velocity and a lower humidity, larger jet droplets and larger film droplets can be released in the bubbly flow regime which contribute to the resuspension rate. This may be the reason why in other tests the resuspension rate was measured higher than in THAI.

6 Validation

AIM was continuously validated on iodine tests of different programs.The complete AIM validation matrix is given in Table 6-1. Details on the performed calculations and the comparison with experimental results can be found in the literature indicated.

An essential contribution to the AIM validation comes from a series of 15 large-scale iodine tests carried out in the 60 m³ vessel of the THAI facility including three multi-compartment tests. Additionally AIM was validated on several RTF (AECL) and CAIMAN (IRSN) experiments. Five of these tests were subject of the International Standard Problem ISP-41 performed in three stages. In recent work AIM-3 was successfully applied to the PHEBUS test FPT1 and on 4 EPICUR tests. Due to the numerous changes in AIM-3 as compared to previous versions, some further tests will be recalculated in future.

Table 6-1: AIM validation matrix

Project (vessel vol.)	**Test**	**Short description**	**AIM-Version**	**Remarks**	**Reference**
CAIMAN (300 l)	CAIMAN 97/02	Steel, painted coupon, 90°C, pH=5, 1 kGy/h	AIM-F1	ISP-41	/BAL 04/
	CAIMAN 01/01	Steel, painted coupon, 110°C, pH=5, 3 kGy/h	AIM-F1	ISP-41	/BAL 04/
	CAIMAN 01/03	Paint, 130-90°C, pH=4-5,5 kGy/h	AIM-F2	External validation AREVA	/BAU 07/
RTF (320 l)	RTF P10T1	Paint, 60°C, pH=4-10, 0.7 kGy/h	AIM-F1	ISP-41	/BAL 04/
	ACE-RTF 3B	Paint, 60°C, pH=5.7-9, 2 kGy/h	AIM-F2	External validation AREVA	/BAU 07/
	PHEBUS-RTF 1	Steel, painted coupon, Gas: 110 °C, pH=5, 1 kGy/h	AIM-F1	ISP-41	/BAL 04/
	PHEBUS-RTF 3	Steel, painted coupon, Gas: 110 °C, pH variation, 1 kGy/h	AIM-K		unpublished
	PHEBUS-RTF 5	Steel, painted coupon, Gas: 70 °C, sump evaporation, pH=5, 1 kGy/h	AIM-K		unpublished
THAI (60 m³)	Iod-6	Iodine/steel	AIM-F2	Evaluation also by AREVA	/WEB 05/, /LAN 08a/,
	Iod-7	Iodine/steel	AIM-F2	Evaluation also	/WEB 05/,

Project (vessel vol.)	**Test**	**Short description**	**AIM-Version**	**Remarks**	**Reference**
				by AREVA	/LAN 08a/,
	Iod-8	Iodine/steel with wall condensation	AIM-F2		/WEB 05/
	Iod-9	2 sumps, mass transfer Sump/atmosphere	AIM-3	SARNET THAI-Circle	/WEB09a/
	Iod-10	Multi-compartment, dry	AIM-F2	Comparison with ASTEC-IODE; ICONE-14	/WEB 05/, /WEB 06/
	Iod-11	Multi-compartment, high humidity	AIM-F2	Comparison with ASTEC-IODE; ICONE-14, proposed for SARNET-2	/WEB 06/
	Iod-12	Multi-compartment with wall condensa-tion	AIM-F2	Comparison with ASTEC-IODE; ICONE-14, proposed for SARNET-2	/WEB 06/
	Iod-13	Iodine/ozone	AIM-F2		/FUN 09a/, /FUN 09b/, /SPE 09/
	Iod-14	Iodine/ozone	AIM-3		/FUN 09a/, /FUN 09b/, /KLE 09b/
	Iod-15	Iodine/paint	AIM-F2, AIM-3	Evaluation also by AREVA	/LAN 08a/, /KLE 09b/
	Iod-16	Iodine/steel	AIM-3	Evaluation also by AREVA	/LAN 08a/, /KLE 09b/
	Iod-17	Iodine/paint	AIM-3	Evaluation also by AREVA	/LAN 08a/, /KLE 09b/
	Iod-18	Steel, humidity varied	AIM-3	Evaluation also by AREVA	/LAN 08a/
	Iod-19	Repetition of Iod-11	AIM-3		/KLE 09b/
	Iod-20	Iodine/paint	AIM-3	Evaluation by AREVA	/LAN 08a/
	Iod-21	Paint, wall condensation		Pre calculation	/KLE 09b/
PHEBUS (10 m³)	FPT1	Integral test with real fission products and dose	AIM-3	Comparison with ASTEC-IODE, for SARNET-PHYMA	/WEB 08/
EPICUR (5 l)	S1-3, S1-4, S1-5, S1-11	Inorganic iodine hydrolysis and radi-olysis in sump	AIM-3	External validation AREVA	/LAN 08b/, /FUN 08/

7 Description of input parameters

The required AIM input parameters and their description are summarized in Table 7-1. The iodine parameters are grouped into four sections:

(1) Steering parameters
(2) Iodine nodalisation, initial and boundary conditions
(3) Iodine injection
(4) General iodine parameters

The format and the exact order of the iodine parameters in the input deck as well as a description of the AIM-3 output is given in the COCOSYS Users's Manual /KLE 09a/. There are also parameters for other models described which are necessary for a complete COCOSYS-AIM input. These parameters concern the thermal hydraulic nodalisation, aerosol behaviour, and engineered systems, e.g. pumps, filters, sprays.

The types of the variables given in Table 7-1 are indicated by *(r), (i), (c)*, which means real number, integer number and character string.

Table 7-1: Input parameter description

Input Parameter (alias in text)	**Description**	**Additional information in Chapter**
(1) Steering parameters		
KEYJOD	Key for the iodine calculation *(i)* 0 no iodine calculation 1 start of iodine calculation; all iodine concentrations are initialized to the specified (input) values. 2 restart with continuation of iodine calculation.	

Input Parameter (alias in text)	Description	Additional information in Chapter
AEJOD	Key to calculate the aerosol behaviour of particulate iodine *(i):* 0 simple aerosol calculation with only sedimentation and a monodisperse particle size for all iodine aerosols (AEROSZ); sedimentation area is ZFAREA (THY input) 1 Well mixed approach for high aerosol concentrations. The aerosol depletion of all iodine aerosols (CsI, IO_3^- and Ag, AgI) is calculated from the depletion rate of the first AERIKA component (core melt aerosol). Agglomeration, condensation on the particles and all deposition processes are implicitly considered.	5.3
	2 Multi-component aerosol calculation. CsI–aerosol is simulated by the first AERIKA component, IO_3^- by the second and the Ag aerosol by the third. This order is fixed. AgI is simulated by using the same depletion rate as calculated for CsI. Additional non–iodine aerosols can be calculated on 4th and higher positions. and higher components. KCOMP ≥ 3 (LPCOND = F) or KCOMP ≥ 4 (LPCOND = T). The CsI, IO_3^- and Ag aerosols and their injections have to be defined in the AERIKA input.	
IJOUT	Key for the AFP specific iodine print output (i). After every IJOUT thermal hydraulic print output an iodine output is generated	
(2) Iodine nodalisation, initial and boundary conditions		
$ZJDNAM_i$	Name of the iodine-zone (c)	
CTYP	Type of the iodine compartment. (c) The available types are: A+S gas-water compartment ATM gas compartment ENV environment compartment **Caution:** For a separate iodine nodalisation the transfer rules have to be considered. The last compartment has to be of type ENV. Only one environment compartment is allowed.	5.1

Input Parameter (alias in text)	Description	Additional information in Chapter
$CZONE_i$	Names of thermal hydraulic zones belonging to the given iodine compartment. (c)	
IRKN	Flag to choose rate and activation energy constant sets for a given compartment. (i) 0 automatic choice using thermal hydraulic results 1 permanently dry conditions 2 permanently wet conditions **Explanation** Two sets of constants are available. The first set is used for dry conditions in the gas phase and the second set for wet conditions (with condensation on walls).	5.2.2
PH	pH value for water pool/sump as function of time. (r)	
FSED	Sump surface area [m^2] as function of time. (r); FSED has to be > 0. Small values (e.g. 1E-15) stop the iodine mass transfer between sump and atmosphere.	
FOFGP ($A_{P,G}$)	Deposition area of epoxy painted surfaces in the gas region [m^2] as function of time. (r)	
FOFGS	Deposition area of steel surfaces in the gas region [m^2] as function of time. (r)	
FOFGB	Deposition area of concrete surfaces in the gas region [m^2] as function of time. (r)	
FOFWP	Deposition area of epoxy painted surfaces in the water region [m^2] as function of time. (r)	
FOFWS	Deposition area of steel surfaces in the water region [m^2] as function of time. (r)	
FOFWB	Deposition area of concrete surfaces in the water region [m^2] as function of time. (r)	
COMP	Initial concentration: Name of iodine species. (c) The available species (component) names are given in Table 2-1	2.2

Input Parameter (alias in text)	Description	Additional information in Chapter
CSPC	Initial concentration: Part of compartment (c): GAS atmospheric part of compartment SUMP sump part of compartment	
VALUE	Initial mass of given iodine component (r). The unit of this value depends on the iodine species (Table 2-1). Components deposited on surfaces have to be given in [mol/m^2] and the concentrations in [mol/l].	2.2
(3) Iodine injection		
CIJCOM	Name of injected iodine component, respectively of the dose rate ('DOSE_RATE') (c). The possible iodine components are given in Table 2-1	2.2
$CIJRATE_i$	Injection rate r (r) as function of time. The unit of the injection rate depends on the injected component CIJCOM: iodine r [mol/s] dose rate r [kGy/h]	
(4) General iodine Parameters		
DZLIM	Maximum iodine time step size [s]. (r) This value is limited to the maximum time step size HMM. **Recommendations:** default 1000 s; should be reduced in multi-compartment calculations if there is an iodine mass balance error.	
S (S_{AG})	Specific surface area of silver particles in the sump (m^2/g); Default value for reactor case is 6.0E-3 m^2/g, following an analysis of PHEBUS-FPT1	3.2.3
ENTRCR	Minimum (critical) sump evaporation rate which activates droplet entrainment (wet resuspension) of the species CsI, IO_3^- and HOI [kg/s]; Default 1.0E–3. (r)	3.4.2

Input Parameter (alias in text)	Description	Additional information in Chapter
CRTHE	Minimum (critical) water height h [m] in a water pool/sump, above which iodine chemistry is calculated. (r) At less water the iodine species are frozen. The value may depend on the individual application. For reactor analyses a height of 1.0E-2 m could be suitable.	5.2.3
ACOND	Minimum specific wall condensation rate for wet conditions. Below this value the conditions are dry. Used with IRKN = 0 only. Recommended value: 1.0E-4 kg/(m²·s)	5.2.2
AGE	Age of Epoxy paint [year]. Used with I^- deposition on immersed paint only. Recommended value: 30 years.	3.2.5
DIO3	Mass median diameter of IO_3^- primary particles. 0.1 µm recommended.	3.4.3, 5.3
SIO3	Standard deviation of log-normal IO_3^- particle size distribution. 1.7 recommended.	3.4.3, 5.3
AEROSZ	Monodisperse particle size [µm] of particulate iodine species (CsI, IO_3^-, AgI and Ag) (r) Used with KAEJOD = 0 only.	5.3
DROPSZ	Monodisperse particle size [µm] of resuspended droplets (r). Used with CsI, IO_3^-, and HOI droplets. Drying of the particles and shrinking are not modelled.	5.3
LMTCAL	Dummy	
KMTGAS	Gas side mass transfer coefficient at the gas / sump interface [m/s] (r). Used to calculate the overall sump/atmosphere transfer for I_2 and CH_3I. Default value 1.4E-3 m/s.	3.4.1
KMTWAS	Water side mass transfer coefficient at the gas / sump interface [m/s] (r). Used to calculate the overall sump/atmosphere transfer for I_2 and CH_3I. Default value 1.0E-5 m/s. May be significantly higher in a strongly mixed sump.	3.4.1

Input Parameter (alias in text)	Description	Additional information in Chapter
F444	Fraction of deposited I_2 onto paint which is washed down immediately into the sump under condensation conditions (r). The fraction (1-F444) stays on the painted surface. Recommended value is 0.68	3.3.3
STOFAC	Stoichiometric factor used for O_3 destruction by I_2 oxidation to IO_x. A value of 3.9 is recommended.	3.3.1
CVTYP	To overwrite default reaction constants. Type of user defined reaction constant (c): BAS1 basis of reaction constant set 1 BAS2 basis of reaction constant set 2 EAKT1 activation energy of reaction constant set 1 EAKT2 activation energy of reaction constant set 2	4, Tab.4-1
I	Number of reaction (i)	
IVAL	User defined value of reaction constant (r). Overwrites the default value.	

8 Literature

/BAL 04/ J. Ball, C Marchand
"ISP-41 – Follow-up Exercise Phase 2
Iodine Code Comparison Exercise against CAIMAN and RTF Experiments"
NEA/CSNI/R(2004)16

/BOR 85/ R. Borkowski
"Untersuchungen des Methyljodides bei schweren Störfällen in Druckwasserreaktoren"
KfK 3968 (1985)

/BAU 07/ M. Bauer, K.-G. Petzold, G. Langrock, "Validierung des Iodmodells in COCOSYS“, AREVA NP , NGPS4/2005/de/0004A, 26. November 2007
and
G. Langrock, M. Bauer, K.-G. Petzold, J. Eyink, F. Funke, "Validierung des Iodmodells in COCOSYS - Beitrag von AREVA NP",
Annual Meeting on Nuclear Technology, May 16.-18., 2006, Aachen

/BEA 87/ E.C. Beahm et al., "Organic iodide formation during severe accidents in light water reactors", Nucl. Technol. 78 (1987) 34 - 41

/BEL 82/ J.T. Bell et al., "Predicted rates of formation of iodine hydrolysis species at pH levels, concentrations, and temperatures anticipated in LWR accidents", NUREG/CR-2900; ORNL-5876 (1982)

/BOS 08/ L. Bosland, F. Funke, N. Girault, G. Langrock, "PARIS project: Radiolytic oxidation of molecular iodine in containment during a nuclear reactor severe accident; Part 1. Formation and destruction of air radiolysis products - Experimental results and modelling",
Nucl. Eng. and Des. 238 (2008) 3542-3550

/BOS 09/ L. Bosland, “ ASTEC V2 code; IODE module: iodine and ruthenium behaviour in the containment”, IRSN, SEMIC – 2009 - 178

/DAP 08/ M. Dapper, M. Bendiab, H.-J. Wagner, M.K. Koch, "Nasse Resuspension, Modellentwicklung der Filmtropfenfreisetzung“, 3. Technischer Fachbericht zum Forschungsvorhaben BMWi 150 1300: Einfluss von Resuspensions-prozessen auf den Quellterm und Beitrag zur an COCOSYS angepassten Modellierung von Wasservorlagen, LEE-47, Lehrstuhl für Energiesysteme und Energiewirtschaft, Ruhr-Universität Bochum, April 2008.

/DIC 99/ S. Dickinson, H. Sims, E. Belval-Haltier, D. Jacquemain, C. Poletiko, F. Funke, Y. Drossinos, E. Krausmann, B. Herrero, T. Routamo, E. Grindon, B.J. Handy, "Kinetics of the uptake of aqueous iodine on silver surfaces", OECD Workshop on Iodine Aspects of Severe Accident Management, Vantaa, Finland, May 18 – 20, 1999.

/DIC 01/ S. Dickinson, H.E. Sims, E. Belval-Haltier, D. Jacquemain, C. Poletiko, F. Funke, S. Hellmann, T. Karjunen, R. Zilliacus, "Organic iodine chemistry" Nuclear Engineering and Design 209 (2001) 193 – 200

/DIC 03/ S. Dickinson, G.M.N. Baston, H.E. Sims, F. Funke, R. Cripps, H. Bruchertseifer, B. Jäckel, S. Güntay, H. Glänneskog, J.O. Liljenzin, L. Cantrel, M.P. Kissane, E. Krausmann, A. Rydl, "ICHEMM Final Synthesis Report", 5th Euratom Framework Programme 1998-2002, Key Action: Nuclear Fission, SAM-ICHEMM-D021, March 2003

/EVA 97/ G.J. Evans et al. "Iodine Behaviour in Containment" Interfacial Transfer of Iodine in Containment ACEX TR-B-05 (1997)

/FUN 96a/ F. Funke, G.-U. Greger, A. Bleier, S Hellmann, W. Morell, "The reaction between iodine and silver under severe PWR accident conditions - an experimental parameter study", OECD Workshop on the Chemistry of Iodine in Reactor Safety, PSI, Würenlingen, Switzerland, June 10 - 12, 1996

/FUN 96b/ F. Funke et al., "Iodine-steel reactions under severe accident conditions in light-water reactors", Nucl. Eng. & Des. 166 (1996) 357-365

/FUN 99/ F. Funke, P. Zeh, S. Hellmann, "Radiolytic oxidation of molecular iodine in the containment atmosphere", OECD Workshop on Iodine Aspects of Severe Accident Management, Vantaa, Finland, May 18 – 20, 1999.
and
F. Funke, P. Zeh, G.-U. Greger, S. Hellmann, "Theoretische und experimentelle Untersuchungen zum Verhalten des Iods bei auslegungs-überschreitenden Ereignissen: Flüchtiges Iod",
Final Report of a project funded by the Bundesminsterium für Bildung, Wissenschaft, Forschung und Technologie (BMBF) in the frame of the Reactor Safety Research program under no. 1501023 (Aug. 99)

/FUN 04/ F. Funke, G.-U. Greger, G. Langrock, T. Kanzleiter, G. Ahrens, K. Fischer, A. Kühnel, G. Poss, H.-J. Allelein, G. Weber, S. Schwarz,
"ThAI-Abschlußbericht Teil 2: Iod-Versuche",
Reaktorsicherheitsforschung - Vorhaben Nr. 150 1218,
Framatome ANP, Erlangen, und Becker Technologies,
Eschborn (April 2004)

/FUN 06/ F. Funke, G. Langrock, T. Kanzleiter, G. Poss, G. Weber, H.-J. Allelein, "Versuchsanlage und Programm zur Untersuchung offener Fragen zum Spaltproduktverhalten im Sicherheitsbehälter - ThAI Phase II, Teil 2: Iod-Versuche“, Abschlussbericht des Vorhabens 1501272 der Reaktorsicherheitsforschung, August 2006,

/FUN 08/ F. Funke, "Testing of the empirical inorganic iodine radiolysis model in AIM using data from the EPICUR tests S1-3, S1-4, S1-5 and S1-11",
AREVA NP NTCR-G/2008/en/0154A, April 2008

/FUN 09a/ F. Funke, G. Langrock, T. Kanzleiter, G. Poss, G. Weber, H.-J. Allelein, "Iodine oxide behaviour in large scale THAI tests", 8th Meeting of the International Source Term Chemistry Interpretation Circle (ISTP-CHEMIC), Petten, April 2, 2009

/FUN 09b/ F. Funke et al.
„Iodine oxides in large-scale THAI tests”
Paper for Nucl. Eng. and Des. in preparation

/FUR 72/ R. Furuichi et al., "Rate of the Dushman reaction at low concentrations, experimental method and temperature coefficient", Inorg. Chem. 11 (1972) 952

/FUR 85/ M. Furrer, R.C. Cripps and R. Gubler
"Measurement of Iodine Partition Coefficient"
Nuclear Technol. 70 (1985) 290-293

/GIR 04/ N. Girault, S. Dickinson, F. Funke, A. Auvinen, L. Herranz, E. Krausmann, "Iodine behaviour under LWR accident conditions: lessons learnt from analyses of the first two Phebus FP tests",,
Nucl. Eng. and Des. 236 (2004) 1293 – 1308

/GIR 08/ N. Girault, L. Bosland
"Analysis of iodine oxide occurrence in Phebus tests"
ISTP project, 6th CHEMIC Meeting, Bergen, NL, 3 April 2008

/GÜN 92/ S. Güntay, R. Cripps
"IMPAIR-3: A Computer Program to Analyze the Iodine Behaviour in Multi-compartments of a LWR Containment"
PSI-Bericht Nr. 128
Paul Scherrer Institut, Würenlingen, Switzerland (1992)

/HEL 96/ S. Hellmann, F. Funke, G.-U. Greger, A. Bleier, W. Morell,
"The reaction between iodine and organic coatings under severe PWR accident conditions - an experimental parameter study", OECD Workshop on the Chemistry of Iodine in Reactor Safety, PSI, Würenlingen, Switzerland, June 10 - 12, 1996

/HOF 95/ W. Hoffmann et al., "Bestimmung von organischen Verunreinigungen in Leichtwasserreaktoren", VGB Kraftwerkstechnik 75 (1995) 814 - 818

/KLE 00/ W. Klein-Hessling, S. Arndt, G. Weber
"COCOSYS V 1.2 User Manual"
GRS-P-3/1 (2000)

/KLE 09a/ W. Klein-Hessling et al.
"COCOSYS V 2.4 User's Manual"
In preparation

/KLE 09b/ W. Klein Hessling et al.
„Gezielte Validierung von COCOSYS und ASTEC sowie generische Anwendungsrechnungen mit diesen Rechenprogrammen", Abschlussbericht des Reaktorsicherheit-Vorhabens RS 1170
GRS-A- report to be published

/LAN 05/ G. Langrock, "PARIS - Overview of the experimental results", 1st meeting of the International Source Term Chemistry Interpretation Circle (ISTP-CHEMIC), Aix-en-Provence, October 20, 2005

/LAN 08a/ G. Langrock, "Konsistente Modellierung der Iod/Stahl- und Iod-Dekontanstrich-Wechselwirkungen in den THAI-Versuchen" (Diplomarbeit Herr Sebastian Ludwiger, Friedrich-Alexander-Universität Erlangen-Nürnberg, August 2007 - März 2008)", Arbeitsbericht AREVA NP, NTCR-G/2008/de/0076A, 06.03.2008

/LAN 08b/ G. Langrock, "Iod-Ablagerung auf Farboberflächen in wässriger Phase" (Diplomarbeit Herr Martin Neumeister, Georg-Simon-Ohm-Hochschule Nürnberg, September 2007 - März 2008)", Arbeitsbericht AREVA NP, NTCR-G/2008/de/0077A, 06.03.2008

/LEM 81/ R.J. Lemire et al., "Assessment of iodine behaviour in reactor containment buildings from a chemical perspective",
AECL-6812 (1981)

/SIM 97/ H.E. Sims, S. Dickinson, G. Evans, J.C. Wren, G. Glowa, "Iodine behavior in containment: the reaction of iodine with surfaces", ACEX-TR-B-06, Draft July 1997.

/SPE 09/ Spengler, C. et al., “Weiterentwicklung der Rechenprogramme COCOSYS und ASTEC, Abschlussbericht des Reaktorsicherheitsforschung-Vorhabens RS 1159“, GRS Köln, 2009

/STE 91/ W. Stephenson, L.M.C. Dutton, B.J. Handy, C. Smedley, "Realistic Methods for Calculating the Releases and Consequences of a Large LOCA", NNC-Report C8141/SYS/002, Issue C, CEC Contract ETNU - 0001/UK, October 1991

/TAN 70/ I.N. Tang and A.W. Castleman, "Kinetics of γ-induced decomposition of methyl iodide in air", J. Phys. Chem. 74 (1970) 3933-3939

/TOT 84/ L.M. Toth et al., "The chemical behaviour of iodine in aqueous solutions up to 150°C - An empirical study of nonredox conditions", NUREG/CR-3514, ORNL-TM-8664 (1984)

/VIK 85/ A.C. Vikis, R. MacFarlane, "Reaction of Iodine with Ozone in the Gas Phase", J. Phys. Chem. 89 (1985) 812

/WEB 05/ G. Weber, "Weiterentwicklung und Validierung des Iodmodells AIM-F2 in COCOSYS Intensivierte Validierung der Rechenprogramme COCOSYS und ASTEC", GRS-A-3299 (2005)

/WEB 06/ G. Weber, H.-J. Allelein, H.-J., F. Funke, T. Kanzleiter, "COCOSYS and ASTEC analyses of iodine multi-compartment tests in the ThAI facility",, ICONE-14: 14th International Conference on Nuclear Engineering, July 17 - 20, 2006, Miami, Florida, USA

/WEB 08/ G. Weber, "COCOSYS and ASTEC comparative analyses of the iodine behaviour in the PHEBUS test FPT1", PHEBUS project CCIC-Meeting, Aix-en-Provence, 16.10.2008

/WEB 09/ G. Weber, L. Bosland, G. Glowa, F. Funke, T. Kanzleiter "ASTEC, COCOSYS, and LIRIC Interpretation of the Iodine Behaviour in the Large-Scale THAI Test Iod-9", ICONE-17, Brussels, Belgium, 12-16 July, 2009

/WRE 99/ J.C. Wren, J.M. Ball, G.A. Glowa, "The chemistry of iodine in containment", Nucl. Technol. 129 (1999) 297-325

/WRE 00/ J.C. Wren, G.A. Glowa, "Kinetics of gaseous iodine uptake onto stainless steel during iodine-assisted corrosion", Nucl. Technol. 133 (2000) 33-49

9 Distribution List

BMWi

Referat III B 4	1 x

GRS-PT/B

Internationale Verteilung	40 x
Projektbegleiter (seh)	3 x

AREVA NP

Hr. Dr. Jürgen Eyink	1 x
Hr. Dr. Ing. Mohammed Bendiab	1 x
Hr. Guillermo Urzua	1 x
Hr. Manfred Erve	1 x
Hr. Axel Nink	1 x
Hr. Dr. Wilfred Morell	1 x
Hr. Dr. Sieghard Hellmann	1 x
Hr. Dr. Gert Langrock	1 x
Hr. Dr. Friedhelm Funke (Autor)	3 x

Becker Technologies

Hr. Gerhard Poss	1 x
Hr. Dr. Karsten Fischer	1 x

Ruhr-Universität Bochum

Hr. Prof. Dr. Marco Koch (LEE)	1 x

RWTH Aachen

Hr. Prof. Dr. Hans-Josef Allelein (LRST)	1 x
Fr. Sara Krajewski (LRST)	1 x

GRS

Geschäftsführung	(hah, stj)	je 1 x
Bereichsleiter	(zir, tes, rot, erv, lim, prg)	je 1 x
Abteilungsleiter	(som, gls)	je 1 x
Projektleiter	(spc)	1 x
Projektbetreuung	(kgl)	1 x
Abteilung 301	(arn, hhm, klh, scz)	je 1 x
Abteilung 302	(trb)	1 x
Informationsverarbeitung	(nit)	1 x
Bibliothek	(Garching, Köln)	je 1 x
Autor	(weg)	7 x

Gesamtauflage: **87 Exemplare**